



POLITECNICO DI TORINO  
Department of Mechanical and Aerospace Engineering  
Master Degree in Automotive Engineering  
A.Y. 2018-2019

Marco Agostini - 253190

# POWERTRAIN COMPONENTS DESIGN

## Engine



---

	Index
<b>1. Crank Slider Mechanism</b>	<b>1</b>
Centered Layout	1
Offset Layout	3
Dynamics	5
Stroke Discussion	6
Centrifugal Inertial Force	6
Forces on the Connecting Rod	7
Torque on the Single Crank	7
Forces and Moment on the Cylinder Block	8
Most Stressed Crank in Multicylinder Engine	8
Engine Degree of Irregularity	9
<b>2. Wrist Pin</b>	<b>11</b>
Design Guidelines	11
Verifications	12
<b>3. Connecting Rod</b>	<b>15</b>
Big Eye	16
Small Eye	16
Materials	16
Load Condition	17
Design Guidelines - Stem	17
Design Guidelines - Small Eye	21
Design Guidelines - Big Eye	22
<b>4. Crankshaft</b>	<b>23</b>
Material	23
Design Guidelines	24
Structural Verification	24
Static Analysis	26
Dynamic Analysis (VI Steps)	26
Dynamic Numerical Analysis (FEA-MBA)	30
<b>5. Bearings</b>	<b>31</b>
Classical Analysis	31
Numerical Coupled FEA-MBA	

---

<b>6. Piston</b>	35
Material	35
Design Guidelines	36
Numerical Analysis	38
Piston Slap	40
<b>7. Cylinder Head</b>	43
Material	43
Cooling	44
Gasket	44
Cover	44
Design Guidelines	45
FEM Analysis	46
<b>8. Cylinder Block</b>	47
Material	49
Liners	49
Design Guidelines	51
Wall	51
Main Cap	52
Liner Support	52
Liner Wall	53
Liner Flange	54
Numerical Analysis (FEA)	54
<b>9. Oil Pan</b>	55
Numerical Optimization – Modal Analysis	55
<b>10. Thermo-Mechanical Fatigue</b>	57
Hysteresis	58
TMF Fatigue Damage	60
Residual Life Estimation	62
Damage Models	62
Basquin-Manson-Coffin	51
Neu-Sehitoglu	52
Chaboche, BMW	52
Skeleton	53
Multiaxial	54

<b>11. Exhaust Manifold</b>	65
Material	65
Design Guidelines	65
Working Condition on the Test Bench	66
Material Behavior	66
Residual Life Estimation – FEA Analysis	67



# 1. Crank Slider Mechanism

Start with crank slider mechanism of single cylinder to find the forces that load all the engine parts. The kinematics studies the position  $x$ , velocity  $\dot{x}$  and acceleration  $\ddot{x}$ , whereas the dynamics is related to forces and torques.

The conversion of reciprocating movement of the piston in rotational motion of the crankshaft is obtained through the so-called crank mechanism:

- The small end of the connecting rod is attached to the piston by means of the wrist pin,
- The big end of the connecting rod rotates with the crankpin
- The crank mechanism transforms the thermal energy of the cylinder charge into mechanical work of the crankshaft.

## Centered Layout

### Position

Starting from the geometrical balance:

$$r \sin \vartheta = l \sin \beta, \quad \lambda = \frac{r}{l} \quad \text{Elongation factor}$$

$$\sin \beta = \lambda \sin \vartheta$$

$$\cos \beta = \sqrt{1 - \sin^2 \beta} = \sqrt{1 - \lambda^2 \sin^2 \vartheta}$$

The **position**  $x_p$  is computed as:

$$x_p = A' O - A O = A' O - A D - D O$$

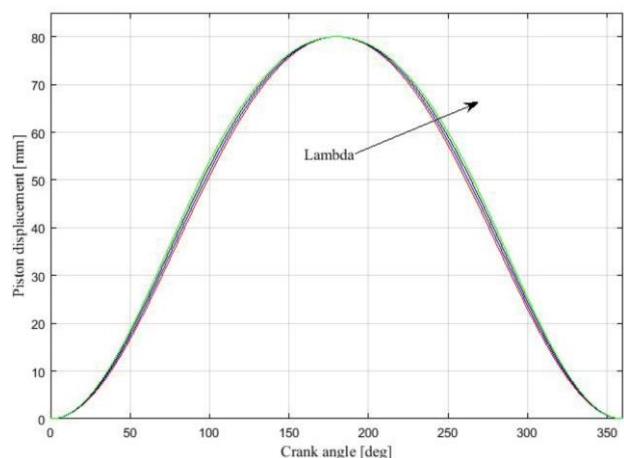
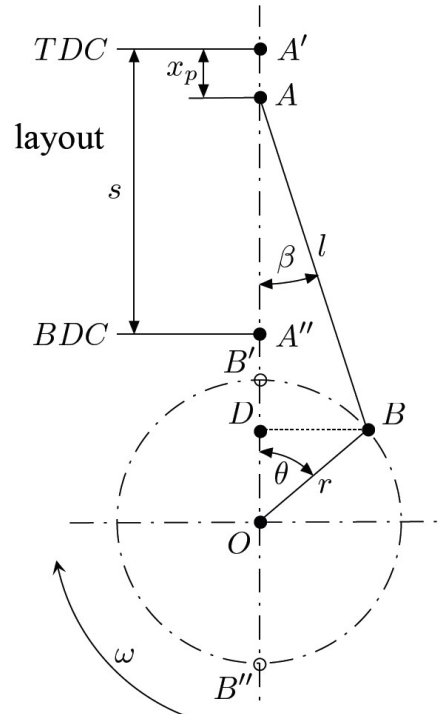
$$x_p = (l + r) - r \cos \vartheta - l \cos \beta$$

$$x_p = r - r \cos \vartheta + l(1 - \cos \beta)$$

$$x_p = r \left[ 1 - \cos \vartheta + \frac{1}{\lambda} - (1 - \cos \beta) \right]$$

$$x_p = r \left[ 1 - \cos \vartheta + \frac{1}{\lambda} \left( 1 - \sqrt{1 - \lambda^2 \sin^2 \vartheta} \right) \right]$$

The higher the Elongation factor  $\lambda$ , the higher the piston displacement.



## Velocity

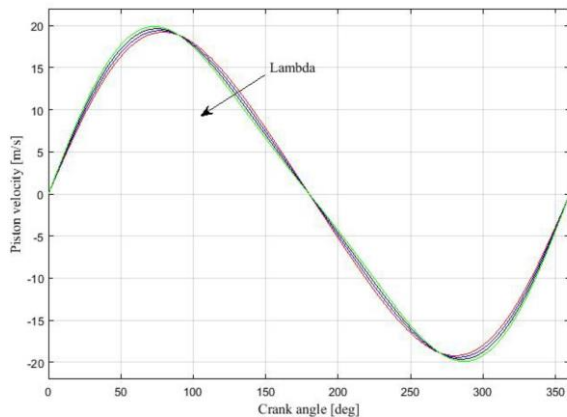
In this way, according to the Elongation Factor  $\lambda$ , the piston displacement increases as  $\lambda$  increases. Once the position  $x_p$  has been defined, then the velocity is the time derivative of the position:

$$v_p = \omega r \left[ \sin \vartheta + \frac{\lambda}{2} \frac{\sin 2\vartheta}{\sqrt{1 - \lambda^2 \sin^2 \vartheta}} \right]$$

As the term  $\lambda^2 \sin^2 \vartheta$  can be neglected with respect to the unit (very low), the centered piston velocity results:

$$v_p = \omega r \left( \sin \vartheta + \frac{\lambda}{2} \sin 2\vartheta \right)$$

The maximum velocity is obtained for  $\cos \vartheta + \lambda \cos 2\vartheta = 0$  which is slightly towards the TDC.



The **mean piston velocity** is equal to:

$$u = 2s \frac{n}{60}$$

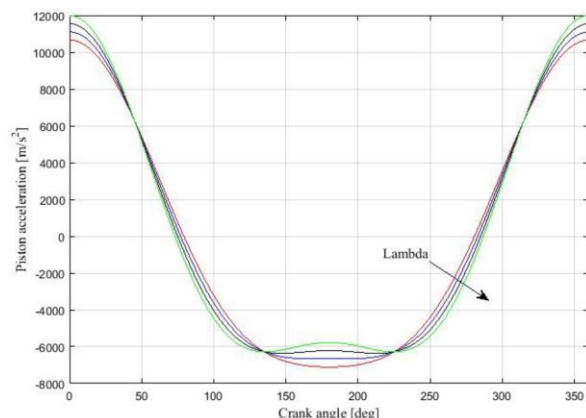
where  $n$  is the engine speed in rpm. This parameter is important since it affects the fluid losses during the gas exchange process.

Increasing  $u$ , inertia pressure increases!!

## Acceleration

Again, by derivating the velocity, one obtain the instantaneous acceleration. By neglecting the term  $\lambda^2 \sin^2 \vartheta$ , one has the approximated piston acceleration:

$$a_p \approx \omega^2 r (\cos \vartheta + \lambda \cos 2\vartheta)$$



- The first-order term is linked to the crank rotation.
- The second-order term is produced by the increase/decrease of the connecting rod obliquity (angle  $\beta$ ) with respect the cylinder axis.
- The second order has double the frequency than the first-order term.

## Offset Layout

### Position

In the offset layout, the cylinder axis does not intersect the center of the crankshaft. The overall offset  $z_o$  is the sum of the displacement  $z_{o,c}$  of the crankshaft axis and the displacement  $z_{o,wp}$  of the wrist pin axis:

$$z_o = z_{o,c} + z_{o,wp}$$

Again, starting from the geometrical balance:

$$D'B = D'D + DB$$

$$r \sin \vartheta = z_o + l \sin \beta$$

- $\lambda = \frac{r}{l}$  Elongation factor

- $\delta = \frac{z_o}{l}$  Adimensional Offset

$$\sin \beta = \lambda \sin \vartheta - \delta$$

$$\cos \beta = \sqrt{1 - \sin^2 \beta} = \sqrt{1 - (\lambda \sin \vartheta - \delta)^2}$$

The position  $x_p$  is computed as:

$$x_p = A'E - AE = A'E - AD - DE$$

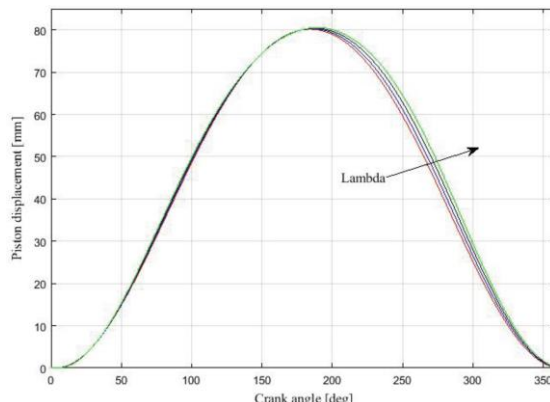
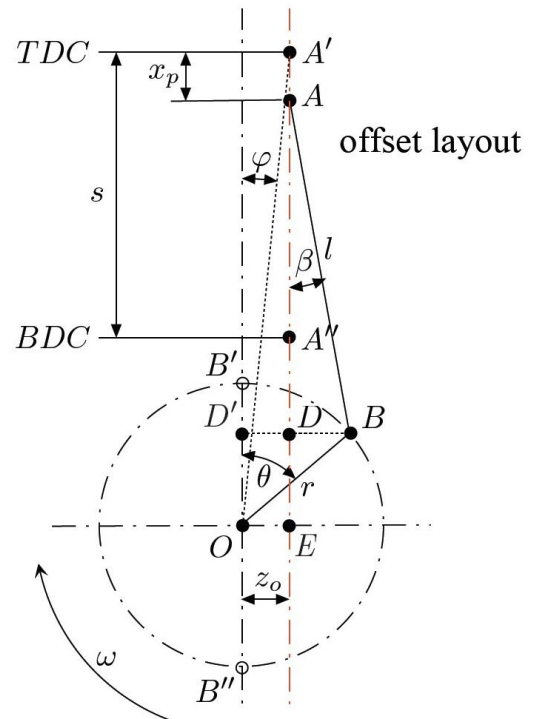
$$x_p = (l + r) \cos \vartheta - r \cos \vartheta - l \cos \beta$$

$$x_p = r - r \cos \vartheta + l(1 - \cos \beta)$$

$$x_p = (l + r) \sqrt{1 - \left(\frac{\delta}{1 + \lambda}\right)^2} - \frac{1}{\lambda} \sqrt{1 - (\lambda \sin \vartheta - \delta)^2} - \cos \vartheta$$

$$x_p = r \left[ \left(1 + \frac{1}{\lambda}\right) \sqrt{1 - \left(\frac{\delta}{1 + \lambda}\right)^2} - \frac{1}{\lambda} \sqrt{1 - (\lambda \sin \vartheta - \delta)^2} - \cos \vartheta \right]$$

In terms of behavior, there are significant changes compared to the centered layout: the higher the elongation factor  $\lambda$ , the higher the piston displacement.



## Velocity

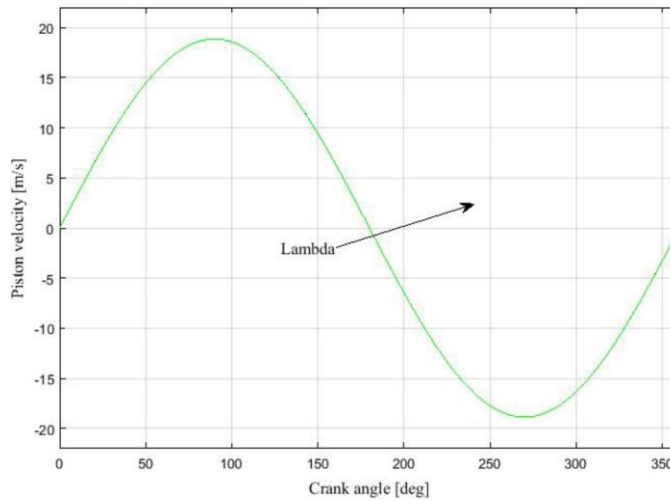
Once the position  $x_P$  has been defined, then the velocity is the time derivative of the position:

$$v_P = \frac{dx_P}{dt} = \frac{dx_P}{d\vartheta} \frac{d\vartheta}{dt} = \frac{dx_P}{d\vartheta} \omega$$

$$v_P = \omega r \left[ \sin \vartheta - \frac{\delta \cos \vartheta}{\sqrt{1 - (\lambda \sin \vartheta - \delta)^2}} + \frac{\lambda}{2} \frac{\sin 2\vartheta}{\sqrt{1 - (\lambda \sin \vartheta - \delta)^2}} \right]$$

As the term  $\lambda^2 \sin^2 \vartheta$  can be neglected with respect to the unit (very low), the centered piston velocity results:

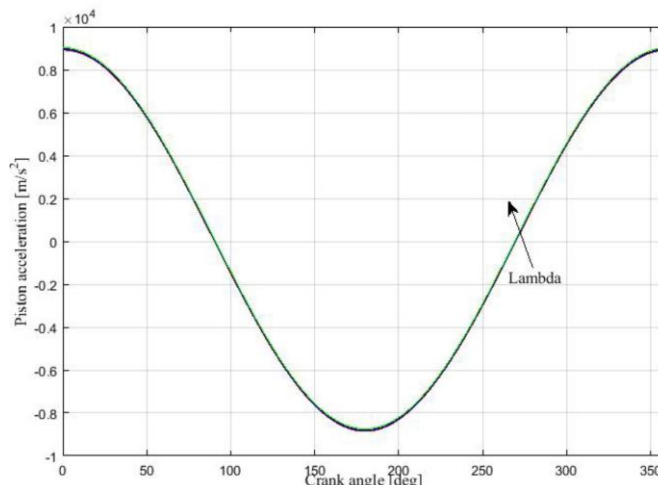
$$v_P = \omega r \left( \sin \vartheta + \frac{\lambda}{2} \sin 2\vartheta \right)$$



## Acceleration

The piston velocity varies during the operative cycle of the engine and it is then possible to obtain the piston acceleration deriving the piston velocity with respect to time:

$$a_P = \omega^2 r \left[ \frac{\sin \vartheta (\lambda \sin \vartheta - \delta)}{\sqrt{1 - (\lambda \sin \vartheta - \delta)^2}} + \frac{\lambda \cos^2 \vartheta}{\sqrt{1 - (\lambda \sin \vartheta - \delta)^2}} + \frac{\lambda \cos^2 \vartheta (\lambda \sin \vartheta - \delta)^2}{\sqrt{(1 - (\lambda \sin \vartheta - \delta)^2)^3}} \right]$$



## Dynamics

The force acting on the crank mechanism can be divided into two contributes:

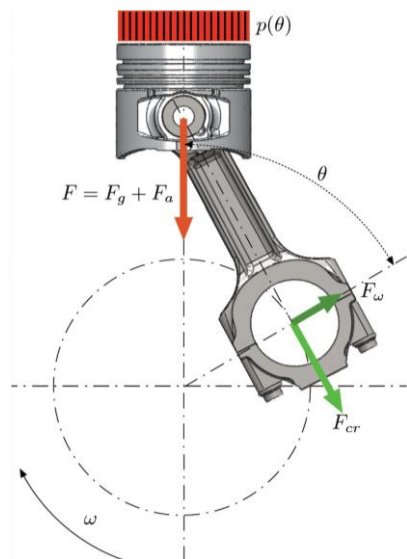
$$F = F_g + F_a$$

- $F_g$  due to gas pressure inside the combustion chamber;
- $F_a$  due to the inertia of the moving parts

The force due to the gas pressure is given by:

$$F_g = [p_g(\theta) - p_0] \frac{\pi D^2}{4}$$

where  $p_g(\theta)$  is the gas pressure as function of the crank angle, and  $p_0$  is the crankcase pressure.

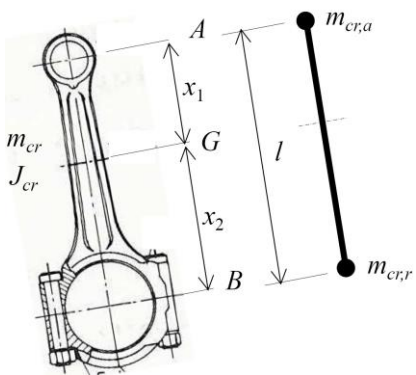


For the inertia force  $F_a$ , it is required to further split the force into two contributions: that caused by masses with reciprocating motion (reciprocating forces) and that given by rotating masses (centrifugal forces):

- Reciprocating forces are directed along the cylinder axis;
- Centrifugal forces passes through the rotating center of the crank (do not influence engine torque).

The connecting rod is simplified as a system with two concentrated masses linked by a rod (with no mass):

- $m_{cr,a}$  is concatenated on the center of the small eye translational motion;
- $m_{cr,r}$  is concatenated on the center of the big eye rotational motion.



$$\begin{cases} m_{cr,a} + m_{cr,r} = m_{cr} \\ m_{cr,a}x_1 = m_{cr,r}x_2 \\ m_{cr,a}x_1^2 + m_{cr,r}x_2^2 + J_0 = J_{cr} \end{cases} \Rightarrow \begin{cases} m_{cr,a} = m_{cr} \frac{x_2}{l} \\ m_{cr,r} = m_{cr} \frac{x_1}{l} \\ J_0 = J_{cr} - m_{cr}x_1x_2 \end{cases}$$

The additional moment of inertia  $J_0$  has no physical meaning (it is always negative) but it is mandatory to guarantee the conservation of the total moment of inertia. For this reason  $J_0$  has the same direction of the angular velocity of the con-rod.

Once the total mass of reciprocating forces (piston group) is calculated, one can obtain the relative force considering a centered crank mechanism and the approximated acceleration:

$$m_a = m_p + m_{wp} + m_{cr,a} \rightarrow F_a = -m_a a_p = -m_a \omega^2 r (\cos \vartheta + \lambda \cos 2\vartheta) = F'_a + F''_a$$

- $F'_a = -m_a \omega^2 r \cos \vartheta$  first-order term
- $F''_a = -m_a \omega^2 r \lambda \cos 2\vartheta$  second-order term (double the frequency, proportional to  $\lambda$ )

$F_a$  is not a rotating vector: direction is fixed in time, amplitude and orientation are functions of the crank angle.

## Stroke Discussion

- **Short Stroke Over-square** Bore > Stroke High spin speed, subjected to low reciprocating inertial force  
Easy to fit bigger valves, lower overall height (motorcycles)
- **Long Stroke Under-square** Bore < Stroke Piston translational velocity reduces, low spin speed but high torque at low regime (industrial application, diesel engines)
- **Square Engine** Bore = Stroke Most used in automotive industry

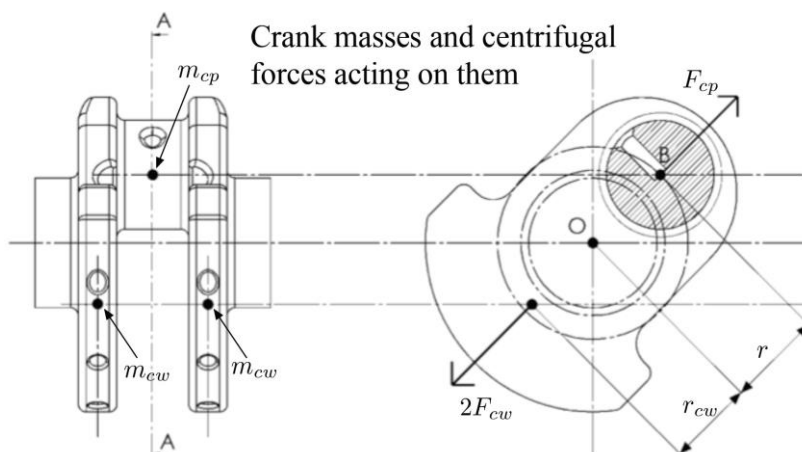
## Centrifugal Inertial Force

Focusing on the crank group, the rotating parts are subjected to the centrifugal force  $F_\omega$ :

$$F_\omega = m_r \omega^2 r$$

where  $m_r$  is composed of the mass of the crankpin  $m_{cp}$  and of the two crankwebs  $m_{cw}$ . These last mass must be reduced since they are placed at a distance  $r_{cw}$  with respect the crank axis whereas  $m_{cp}$  lies on the axis. To reduce the crankweb mass, one exploits the equality of static moments:

$$m_{cw,red} = m_{cw} \frac{r_{cw}}{r}$$



The total rotating mass is then:

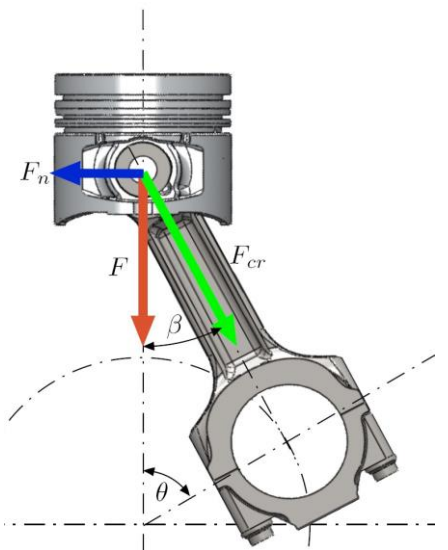
$$m_r = m_{cp} + 2m_{cw,red} + m_{cr,r}$$

The correspondent inertial centrifugal force  $F_\omega$  is a rotating vector with constant amplitude which passes through the axis of rotation of the crank. The horizontal and vertical component are:

- $F_{\omega,h} = F_\omega \sin \vartheta$
- $F_{\omega,v} = F_\omega \cos \vartheta$

## Forces on the Connecting Rod

- $F$  is always directed along cylinder axis:  $F = F_g + F_a$
- The inertia force  $F_a$  is composed of the contribution of the alternating mass, causing  $F_a'$  and  $F_a''$ , and rotational mass, producing  $F_\omega$ .
- $F$  can be decomposed into a normal component  $F_n$  and a component along the con-rod  $F_{cr}$ .
- $F_n$  represents the thrust force on the wall of the liner whereas  $F_{cr}$  is the thrust force on the connecting rod. Force  $F_{cr}$  is actually generating the engine torque.



$$F_{cr} = \frac{F}{\cos \beta} = \frac{F}{\sqrt{1 - \lambda^2 \sin^2 \vartheta}}$$

## Torque on the Single Crank

The force  $F_{cr}$  acting along the con-rod has an arm  $d$  with respect the crankshaft axis, so that the developed torque is:

$$M = F_{cr}d = F_{cr}r \sin(\vartheta + \beta) = \frac{F}{\cos \beta} r \sin(\vartheta + \beta)$$

The torque can also be rewritten as function of the force  $F$  by substituting the  $\beta$  functions:

$$M = Fr \left( \sin \vartheta + \frac{\lambda \sin \vartheta \cos \vartheta}{\sqrt{1 - \lambda^2 \sin^2 \vartheta}} \right)$$

As usual, by neglecting  $\lambda^2 \sin^2 \vartheta$  with respect the unit, the torque on the single crank reduces to:

$$M = Fr \left( \sin \vartheta + \frac{\lambda}{2} \sin 2\vartheta \right)$$

## Forces and moment on the Cylinder Block

The gas pressure inside the cylinder and the inertial forces transfer forces to engine block.

These forces are countered by engine mounts. At the center of the Big Eye (point B), the force  $F_{cr}$  hits the line of action of the centrifugal force  $F_\omega$  that acts on the rotating mass.

Thus, here  $F_{cr}$  and  $F_\omega$  generate an horizontal and vertical force,  $F_h$  and  $F_v$ , acting on the main bearing and consequently on the cylinder block.

- $F_h = F_{cr} \sin \beta + F_\omega \sin \vartheta$
- $F_v = F_{cr} \cos \beta + F_\omega \sin \vartheta$

Considering also the normal force (oriented horizontally) and the gas pressure (oriented vertically), then the overall load on the engine block is:

- |  |  |
|--|--|
| <ul style="list-style-type: none"> <li>• <math>F_H = F_h - F_n = F_\omega \sin \vartheta</math></li> <li>• <math>F_V = F_v - F_g = F_a - F_\omega \cos \vartheta</math></li> </ul> | Only depends on centrifugal force<br><br>Depends on both reciprocating and centrifugal forces. |
|--|--|

Also, the block is balanced by a counterclockwise equilibrium moment:

$$M_e = F_n x(\vartheta) = F_n (\cos \beta + r \cos \vartheta)$$

By developing this expression and neglecting  $\lambda^2 \sin^2 \vartheta$ , one obtains:

$$M_e = Fr \left( \sin \vartheta + \frac{\lambda}{2} \sin 2\vartheta \right)$$

This is equal and opposite to the instantaneous single crank torque and it is proportional to the reciprocating inertial force and the gas pressure (since it depends on  $F$ )

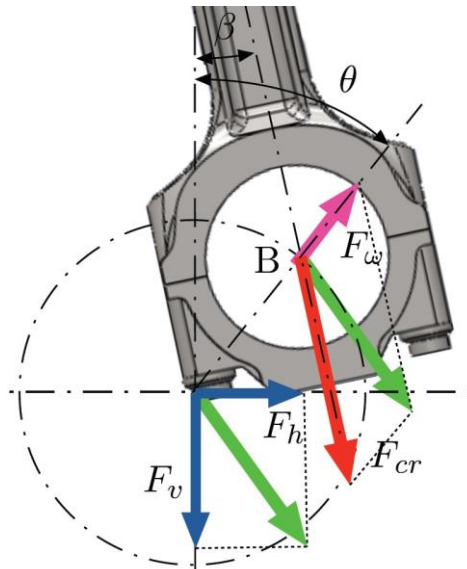
## Most Stressed Crank in Multicylinder Engine

In multi-cylinder engines, the trend of each force and moment computed for the single-cylinder engine has to be superimposed by respecting the engine firing order (FO) to obtain the correct time and space.

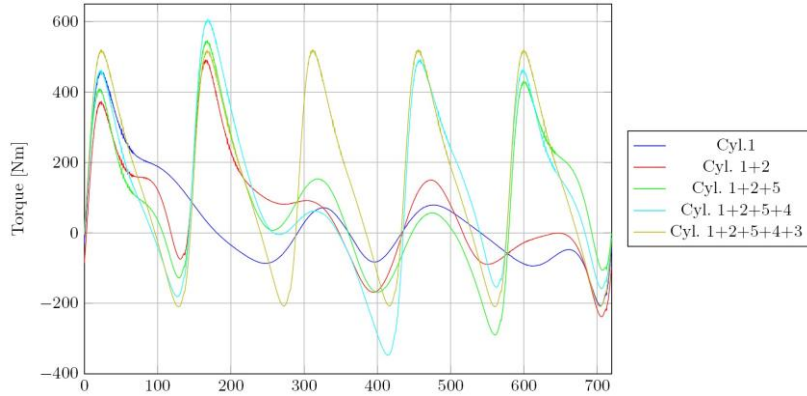
The stress on a specific crank is not solely due by the stress due to the piston connected with that specific crank but also by the presence of the other cranks.

To identify the most stressed crank, the engine torque acting on each “single-cylinder” has to be computed, and the trends of all cylinders have to be added starting from the first cylinder until the last one indicated by the FO:

1. the engine torque acting on each “single-cylinder” is computed and reported on the same graph, respecting the given FO



2. by respecting the FO, the engine torques related to each “single-cylinder” are added together starting from the first cylinder (1) until the last one
3. Finally, as the curve given by the sum of the engine torques of cylinders reaches the maximum highest value, the most stressed crank is that for which the curve reaches the maximum, cylinder 4 in this case.



## Engine Degree of Irregularity

The engine degree of irregularity is the ratio between the maximum and the average engine torque. The higher the number of cylinders, the lower the irregularity.

The crankshaft acceleration is not constant, the power is fluctuating: the objective of the flywheel is to smooth down the acceleration of the crankshaft.

The **Kinematic Irregularity**  $\delta$  parameter is defined as:

$$\delta \stackrel{\text{def}}{=} \frac{\omega_{max} - \omega_{min}}{\omega_{avg}} \leq 1\%, \quad \omega_{avg} = \frac{\omega_{max} + \omega_{min}}{2}$$

This value of the kinematic irregularity set the limit to the maximum allowed speed fluctuation.

The dimensioning analysis of the flywheel is based upon the **engine shaft dynamic equilibrium** equation:

$$M_s(\theta) - M_r(\theta) = \mathcal{J} \frac{d\omega}{dt}$$

where:

- $M_s(\theta)$  shaft momentum as function of crank angle  $\theta$ ,
- $M_r(\theta)$  resistant momentum as function of crank angle  $\theta$ ,
- $\mathcal{J}$  overall engine inertia:  $= \mathcal{J}_{engine} + \mathcal{J}_{flywheel} + \mathcal{J}_{transmission} + \mathcal{J}_{user}$ ,
- $\omega$  engine angular velocity.

The integration of the momentum along the engine cycle is equal to the work, thus:

$$W_s(\vartheta_{max}) - W_r(\vartheta_{max}) = \mathcal{J} \frac{\omega_{max}^2 - \omega_0^2}{2}$$

**I Irregularity Parameter - Kinematic**

$$\Delta W_{max} = \max(W_s - W_r) = \frac{J}{2} \cdot (\omega_{max}^2 - \omega_0^2)$$

In the same way, considering the minimum crankshaft speed  $\vartheta_{min} = \vartheta(\omega = \min)$ , one has:

**II Irregularity Parameter - Kinematic**

$$\Delta W_{min} = \min(W_s - W_r) = \frac{J}{2} \cdot (\omega_{min}^2 - \omega_0^2)$$

The dynamic irregularity  $\xi$  is defined as:

$$\xi = \frac{\mathcal{J}}{\text{imep} \cdot V} \cdot \frac{(\omega_{max} + \omega_{min})(\omega_{max} - \omega_{min})}{2}$$

To satisfy the kinematic irregularity requirements, the velocity term considers the parameter  $\delta$ :

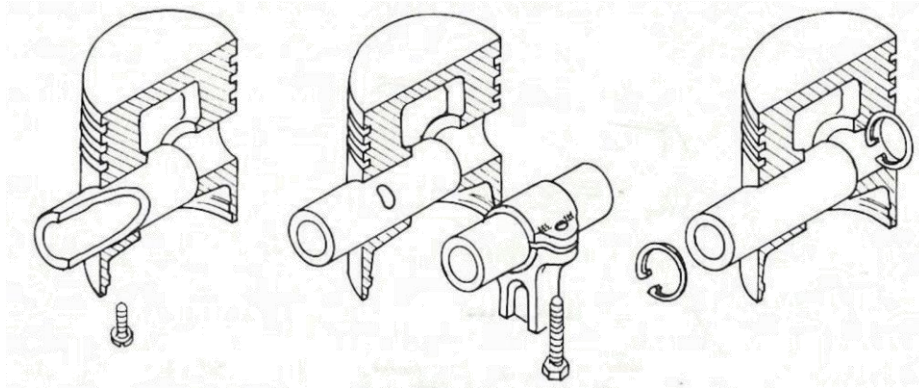
$$\omega_{max} - \omega_{min} = \delta \cdot \omega_{avg}$$

**III Irregularity parameter - Dynamics**

$$\xi = \frac{\mathcal{J}\delta\omega_{avg}^2}{\text{imep} \cdot V}$$

## 2. Wrist Pin

The wrist pin is the connecting element between the piston and the connecting rod. To reduce its mass, its geometry is a hollow cylinder with tapered ends, and thicker in the middle. It is kept in position by snap metal rings inserted into grooves of the piston hub.



Two different configuration can be adopted:

- Fixed pin      Low stressed engine, fixed with respect the small eye of the conrod.
- Floating pin    Medium to high stressed engine, free to rotate compared to the small eye by means of bushings.

Suitable materials must face high fatigue resistance and good surface hardness:

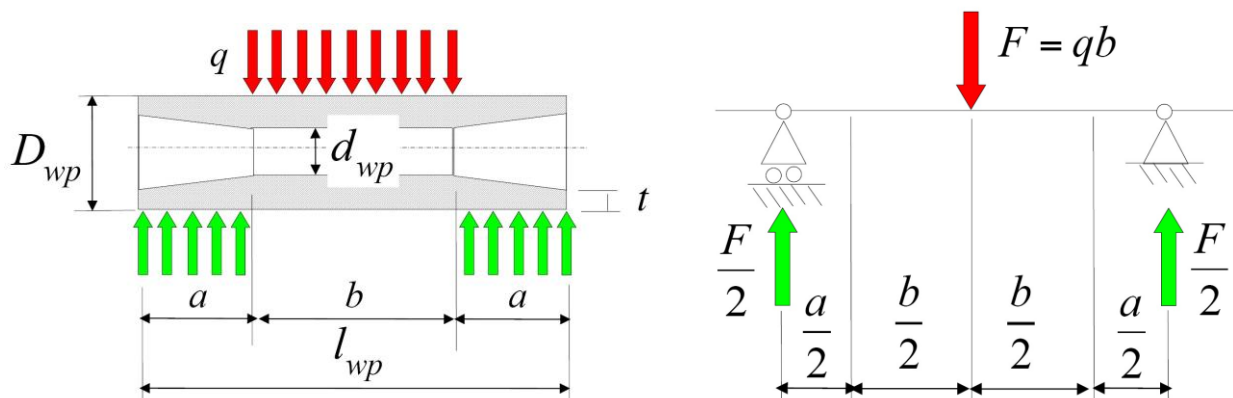
- NiCr               $R_m = 1500 \text{ MPa}$ , hardness up to 240 HB
- Croma             hardness up to 270 HB

## Design Guidelines

The pin is modeled as a beam with 3 distributed load: one external load and the two constraint reactions.

The value of the external force  $F$  depends on the type of verification:

- Static               $F$  is given by the maximum gas compression, inertial force are neglected
- Fatigue             $F$  is a function ranging between  $F_{max}$  and  $F_{min}$

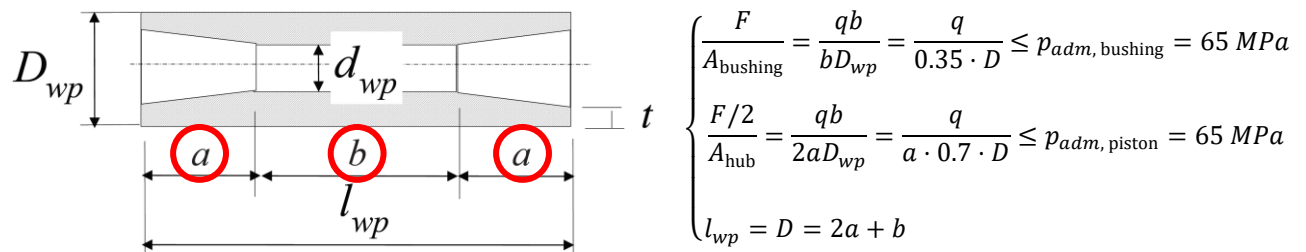


## First attempt design

First consider a sample pin with:

- Pin length is equal to the Bore  $l_{wp} = D$
- Outer diameter equal to 35% of the bore  $D_{wp} = 0.35 D$
- Inner diameter equal to 40% of the bore  $d_{wp} = 0.40 D$
- Thickness 50% of the inner diameter  $t = 0.5 d_{wp}$

Then, one has to find lengths  $a$  and  $b$  by superimposing a contact pressure of 65 MPa



## Verifications

The properties to be verified are **bending**, **shear** and **ovalization**.

### Bending

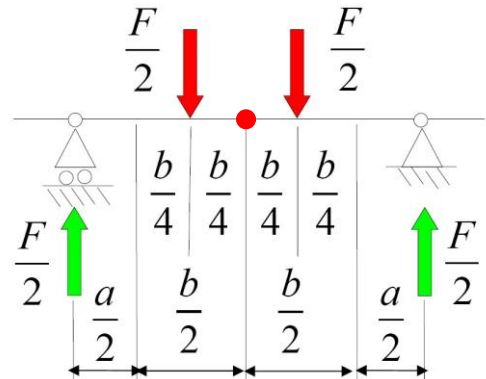
Maximum bending moment  $M_b$  is in the wrist pin midspan:

$$M_b = \left[ \frac{F}{2} \left( \frac{a}{2} + \frac{b}{2} \right) \right] - \left[ \frac{F}{2} \cdot \frac{b}{4} \right]$$

$$M_b = \frac{F}{2} \left( \frac{2a + b}{4} \right)$$

$$M_b = \frac{F}{8} l_{wp} = \frac{qb}{8} l_{wp}$$

The corresponding **bending stress** is:



$$\sigma_b = \frac{M_b}{W_{b,wp}}$$

### Shear

Indicating with  $S_{wp}$  the static moment of area of the wrist pin, the shear stress is:

$$\tau = \frac{F \cdot S_{wp}}{2bI_{wp}}$$

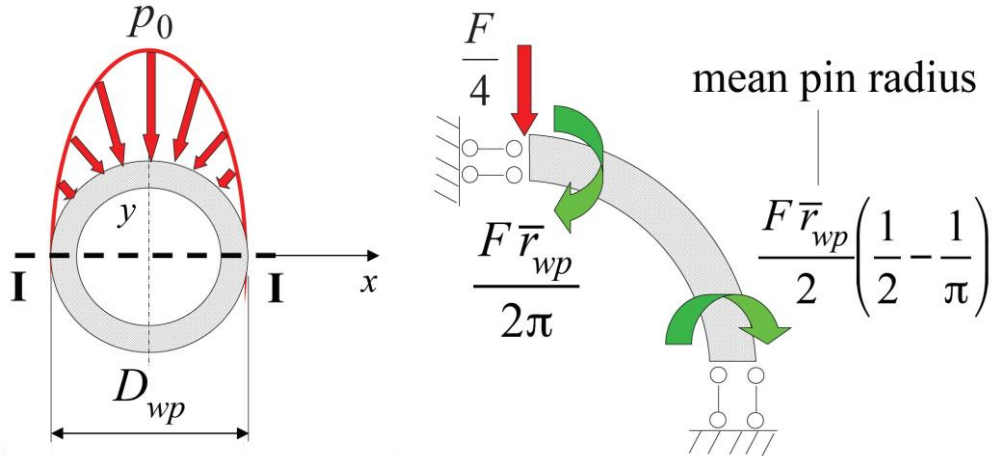
where  $I_{wp}$  is the moment of inertia of the pin in its inflection plane.

### Ovalization

For the ovalization analysis, the wrist pin is modeled as an arc loaded by a pressure distribution acting on the semi-circumference:

$$p = p_0 \sin^2 \varphi, \quad 0 < \varphi < \pi$$

and the piston hubs are assumed rigid.



The analysis is performed according to the *Curved Beam Theory* of a quarter of arc loaded by the external force  $F/4$  and constrained by reactions. The **ovalization moment** is:

$$M_{ov(\pi/2)} = \frac{F \bar{r}_{wp}}{2} \frac{1}{\pi}, \quad \varphi = \frac{\pi}{2}$$

$$M_{ov(0,\pi)} = \frac{F \bar{r}_{wp}}{2} \left( \frac{1}{2} - \frac{1}{\pi} \right), \quad \varphi = 0, \pi$$

The correspondent **ovalization stress** is then:

$$\sigma_{ov} = \frac{M_{ov}}{W_{wp}} = \frac{24 \cdot M_{ov}}{l_{wp} (D_{wp} - d_{wp})^2}$$

### Equivalent Stress

Now it is possible to compute  $\sigma_{eq}$  according to Von Mises in the midspan section of the wrist pin as the combination of the shear and ovalization stresses:

$$\sigma_{eq} = \sqrt{\sigma_{ov(0,\pi)}^2 + 3\tau^2}$$

We compare  $\sigma_{eq}$  with  $\sigma_b$  and the final inner and outer diameters of the pin are computed according to the maximum between  $\sigma_{eq}$  and  $\sigma_b$ :

$$\max(\sigma_{eq}, \sigma_b) \leq \sigma_{adm,wp} \rightarrow D_{wp}, d_{wp}$$

Ovalization also faces lubrication problem, therefore it is required to verify the ovalization also in these limits. These verifications are performed over the **longitudinal** and **transversal** deformation.

### Longitudinal displacement

The wrist pin maximum longitudinal displacement is computed through Structural Mechanics Theory:

$$f = \left(1 - \frac{b}{2(a+b)}\right) \frac{(a+b)^3 F}{48EI_{wp}} \leq f_{adm}$$

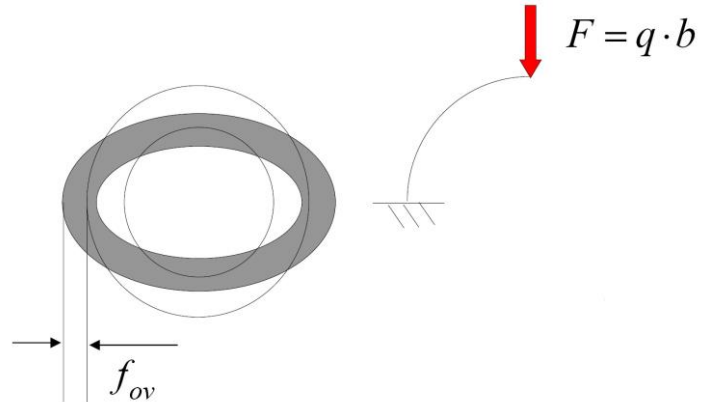
where  $f_{adm}$  is given by CFD computations.

### Transversal displacement

The wrist pin maximum transversal displacement is:

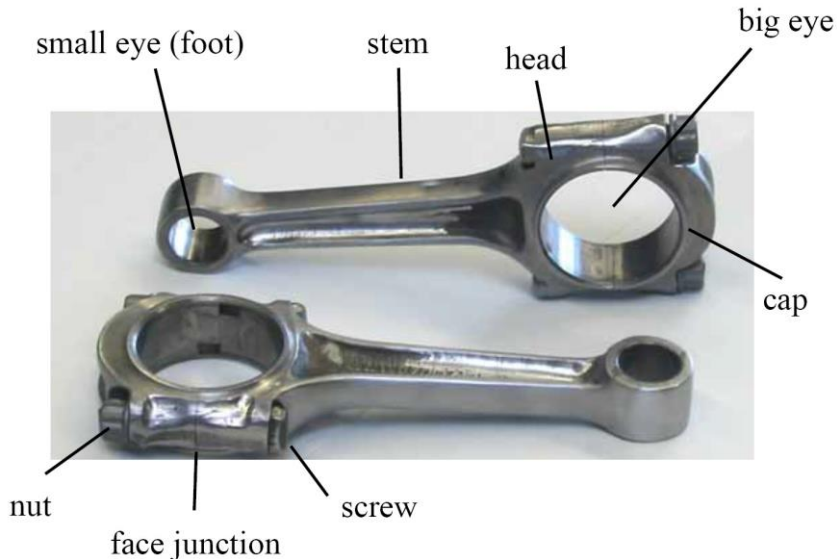
$$f_{ov} = \frac{4F\bar{r}_{wp}^3}{l_{wp}(D_{wp} - d_{wp})^3 E} \leq \delta_{min}$$

where  $\delta_{min}$  is the minimum tolerance assumed for the bushing.



### 3. Connecting Rod

The con-rod is the element that actually converts the alternating motion of the piston group into the rotary motion of the crankshaft. Its design also deeply affects the overall dynamic behavior of the engine. Indeed, the conrod limits the maximum engine speed and creates important transversal load on the liner. The con-rod is composed of:

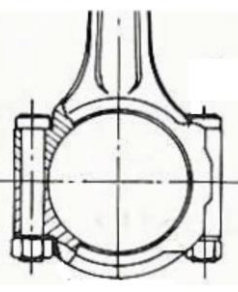
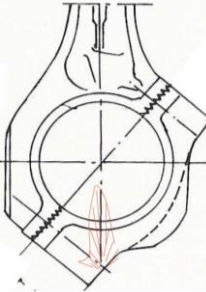


The most stressed part is the stem: it must react to bending and compressive action. Its cross section is usually optimized in terms of weight and stress distribution by using a T geometry. The two possible layout are:

I-Rod Stem	H-Rod Stem
 <ul style="list-style-type: none"> <li>- The stem face is placed in the plane of reciprocating motion.</li> <li>- Low cost solution, high production numbers</li> <li>- Obtained through molding or casting</li> <li>- Good response to whiplash (high moment of inertia)</li> <li>- Not comfortable housing of the nuts, meaning high stress concentration due to the countersink.</li> </ul>	 <ul style="list-style-type: none"> <li>- The stem face is placed perpendicularly to the reciprocating motion</li> <li>- High cost solution</li> <li>- Obtained through machining</li> <li>- Great response in whiplash for high speed engine (short length of the stem)</li> <li>- Housing of nuts is simplified and stress concentration is reduced.</li> </ul>

## Big Eye

The main characteristic of the big eye is the face junction which can be orthogonal or inclined.

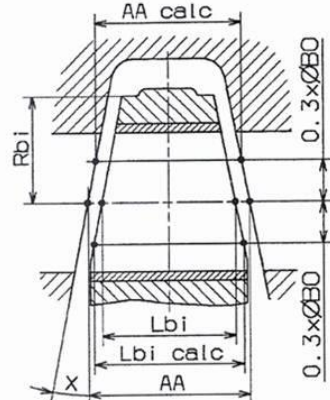
Orthogonal Face Junction	Inclined Face Junction
 <ul style="list-style-type: none"> <li>- The plane of separation between head and cap is placed at 90° with respect to the longitudinal stem axis.</li> <li>- Most used solution.</li> </ul>	 <ul style="list-style-type: none"> <li>- To reduce the transversal dimension of the big eye, the cap is inclined of 30-45° (used for V-engines).</li> <li>- Maximum stress is concentrated on the cap.</li> </ul>

In both solution it is fundamental to avoid shear stress on the screws! For this purpose, the screws are centered with calibrated diameters, dowel or serration.

## Small Eye

The small eye is a pipe drilled perpendicular to the axis of the wrist pin that also includes the lubricant oil adduction. The sides of the small eye can be:

- parallel in medium stressed engines,
- converging in high stress engines so to allow thermal expansion. Further benefits are obtained from the lower reciprocating masses and hence the stress on the con-rod.



## Materials

The material choice depends on the overall mass and strength but also on the manufacturing process:

- |                  |   |
|------------------|---|
| • Cast Iron      | most economical solution, high production numbers                   |
| • Hardened alloy | expensive since require hot forging. Used for high stressed engines |
| • Ti-alloy       | for racing application  |
| • Al-alloy       | for low stressed engines only                                       |

On the finished component, a shot-peen treatment is done to increase residual stress and improve fatigue up to 25%

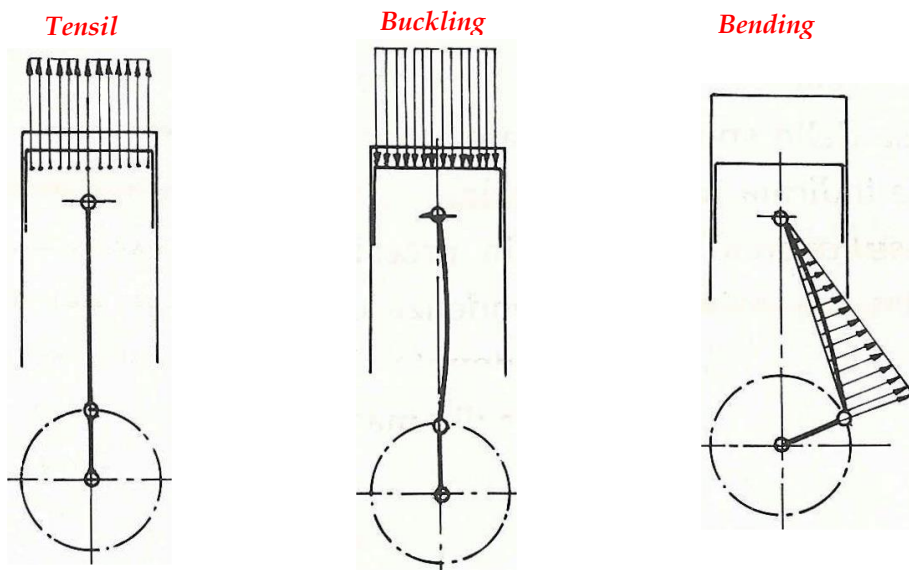
## Load Conditions

The loads acting on the con-rod are **gas pressure** and **inertial forces**. However, it is preferable to consider:

- Starting condition      gas pressure @ maximum torque only
- Operating condition    inertial forces @ maximum speed only (maximum tensile force at TDC)

In the following, consider specific loads:

- **Tensile load**                due to the inertial forces evaluated when pointing towards TDC
- **Buckling load**             due to the maximum compressive force of the gas pressure at TDC or BDC
- **Bending load**              due to the whiplash from the acceleration in the roto-translational motion.  
Fundamental for sizing the bushes in the eyes.



## Design Guidelines - Stem

1. Define the cross section of the stem as the area under which the maximum compressible load is acting:

$$A_{cr} = \frac{F \cdot S}{R_{p0.2}}$$

- $F$       max force between as at TDC and inertial force at BDC
- $S$       safety factor, commonly 1.5
- $R_{p0.2}$     yield strength

2. Verify the tensile load on the evaluated area:

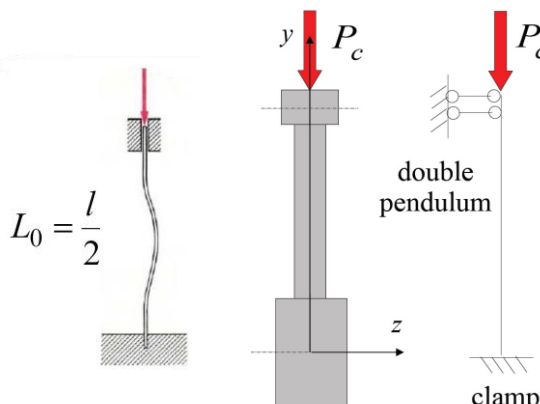
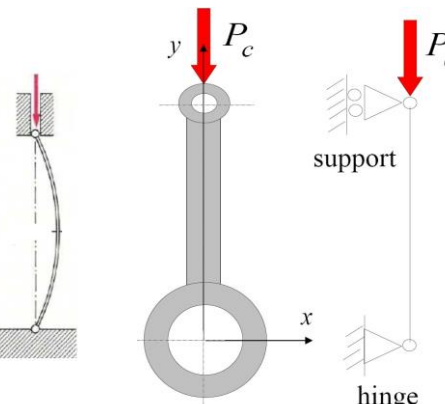
$$\sigma_t = \frac{F_{a,max}}{A_{cr}} = \frac{m_a \cdot a_{p,max}}{A_{cr}} \leq R_{p0.2}, \quad m_a = m_p + m_{wp} + m_{cr,a}$$

3. Verify the **buckling** elastic instability condition by modeling the conrod as a beam undergoing a compressive load. The buckling planes are two both parallel to the con-rod axis:

- one passes for the big eye axis
- the other is perpendicular to the previous one.

Since the buckling planes are two, then also the models are two. Considering  $y$  as the axis of the con-rod and  $z$  the axis of the big eye, then the reference planes are:

- $zy$  containing the wrist pin axis
- $xy$  frontal plane perpendicular to the wrist pin axis

<b><math>zy</math> plane</b>	<b><math>xy</math> plane</b>
 <p><math>L_0 = \frac{l}{2}</math></p>	 <p><math>L_0 = l</math></p>

- Model with one free axial degree of freedom.

- Free length  $L_0$  is equal to half the distance between the center of the two eyes, that is the half length of the con-rod.

- Model with one support and connected to a hinge on the other end.

- Free length  $L_0$  is equal to the distance between the center of the two eyes, that actually the length of the con-rod.

- Since  $L_0 = l$  than the plane  $xy$  is most dangerous for the instability! Use *Euler Equation* to compute the **critical buckling load**:

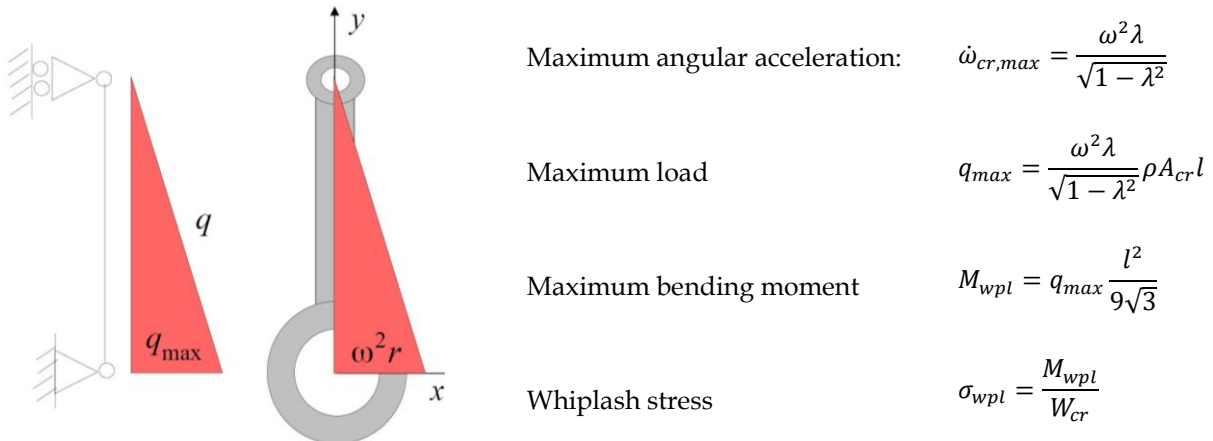
$$P_c = \frac{\pi^2 EI_{cr}}{l^2}$$

For the verification, the maximum force on the stem has to be lower than the critical load:

$$F < P_c$$

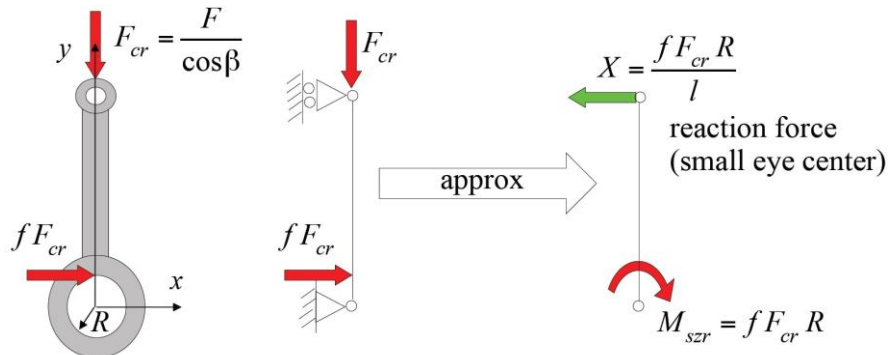
- By imposing this verification, it is possible to get the best  $A_{cr}/I_{cr}$  ratio of the stem cross section.

4. Verify the stem **bending** due to whiplash effect. The acceleration of the con-rod has triangular distribution with null value at the center of the small eye and maximum value at the center of the big eye. From the crank-slider mechanism, the maximum angular acceleration is obtained for  $\vartheta = 90^\circ$



Where  $W_{cr}$  is the bending resistance modulus of the most stressed section of the stem.

5. Verify the **bending due to the seizure of bushing** in the big eye. The bending moment is approximated to a triangular distribution with maximum value in the big eye.



The correspondent stress is computed as:

$$\sigma_{szr} = \frac{f F_{cr} R}{W_{cr} \sqrt{3}}, \quad f = \text{friction coefficient}, \quad R = \text{bushing radius}$$

6. Verify that the **total equivalent stress** is lower than the admissible:

$$\sigma_{eq} = \sigma_t + \sigma_{wpl} + \sigma_{szr} \leq \sigma_{adm}$$

where  $\sigma_{adm}$  is given by the connecting rod material.

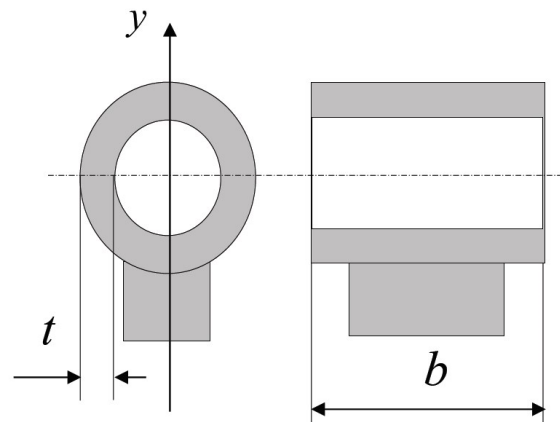
7. For **Fatigue**, use Haigh Diagram without considering the seizure.

To sum up, the stem design is made of 7 steps:

1.	Find the cross section of the stem	$A_{cr}$	$A_{cr} = \frac{F \cdot S}{R_{p0.2}}$
2.	Verify the tensile stress	$\sigma_t$	$\sigma_t = \frac{F_{a,max}}{A_{cr}} \leq R_{p0.2}$
3.	Verify the buckling in $xy$ plane	$P_c$	$P_c = \frac{\pi^2 EI_{cr}}{l^2}, \quad F < P_c$
4.	Compute the whiplash stress	$\sigma_{wpl}$	$\sigma_{wpl} = \frac{M_{wpl}}{W_{cr}}$
5.	Compute the bending stress due to seizure	$\sigma_{szr}$	$\sigma_{szr} = \frac{f F_{cr} R}{W_{cr} \sqrt{3}}$
6.	Verify the total equivalent stress	$\sigma_{eq}$	$\sigma_{eq} = \sigma_t + \sigma_{wpl} + \sigma_{szr} \leq \sigma_{adm}$
7.	Verify Fatigue though Haigh Diagram		

## Design Guidelines – Small Eye

The small eye is modeled as thin tube which is subjected to the alternate inertial force. Usually, only the circumferential stress are considered, however, for small verifications, also the force fitting the bushing and the curvature of the small eye must be considered



<b>1. Circumferential stress</b>	$\sigma_{circ}$	$\sigma_{circ} = \frac{F_{a,max}}{2bt}$	
<b>2. Force fitting the bushing</b>	$\sigma_{fit}$	$\sigma_{fit} = p \frac{D_e^2 + D_c^2}{D_e^2 - D_c^2}$ <p><math>p</math> is the interference pressure,  <math>D_e</math> and <math>D_c</math> are respectively the      small eye outer and inner      diameter (pitch)</p>	
<b>3. Curvature of the small eye</b>	$\sigma_{curv}$	$\sigma_{curv} = \frac{M_{max}}{W_{se}}$ <p><math>M_{max}</math> is the maximum bending      moment,  <math>W_{se}</math> is the bending resistance      modulus of the small eye.</p>	

The total equivalent stress acting in the most stressed section of the small eye is the summation of circumferential, bushing fitting force and curvature stresses:

$$\sigma_{eq} = \sigma_{circ} + \sigma_{fit} + \sigma_{curv} \leq \sigma_{adm}$$

where  $\sigma_{adm}$  is given by the connecting rod material.

## Design Guidelines - Big Eye

The big Eye is divided into cap and head.

### CAP

The cap can be modeled as a supported beam subjected to a concentrated force in the middle, equal to the maximum inertial force.

$$F_a = (m_p + m_{wp} + m_{cr,a})\omega^2 r(1 + \lambda) + m_{cr,r}\omega^2 r$$

The corresponding maximum bending stress is:

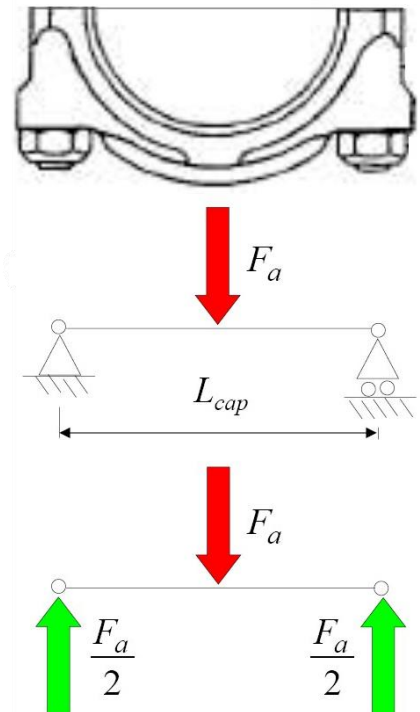
$$\sigma_{cap} = \frac{\frac{F_a}{2} \cdot \frac{L_{cap}}{2}}{W_{cap}}$$

where  $L_{cap}$  is the distance between screws and  $W_{cap}$  is the bending resistance modulus of the cap middle section.

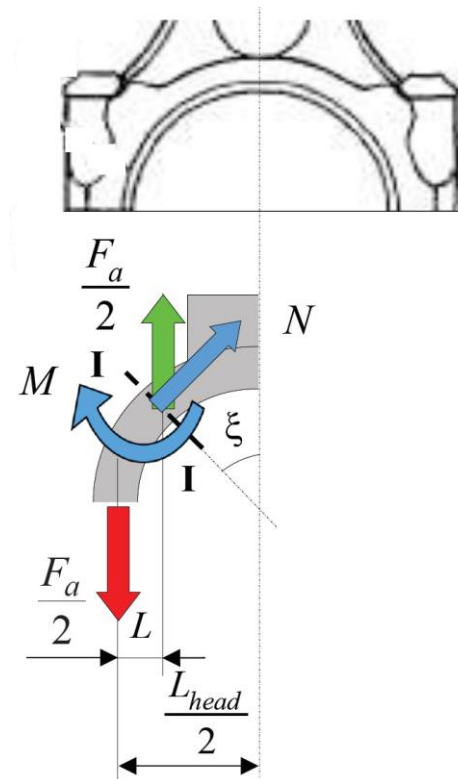
As usual the cap verification is:

$$\sigma_{cap} \leq \sigma_{adm}$$

where  $\sigma_{adm}$  is given by the connecting rod material.



### HEAD



The head can be modeled as a curved beam subjected to the same inertial force. Through the Curved Beam Theory, the involved forces are:

$$N = \frac{F_a}{2} \sin \xi$$

$$M = \frac{F_a}{2} L$$

The total equivalent stress acting in the most stressed section of the head is the summation of the tensile and bending stress:

$$\sigma_{eq,head} = \frac{N}{A_{head}} + \frac{M}{W_{head}} \leq \sigma_{adm}$$

where  $A_{head}$  is the area of the most stressed parts (related to tensile) and  $W_{head}$  is the bending resistance modulus of the head.

Again,  $\sigma_{adm}$  is given by the connecting rod material.

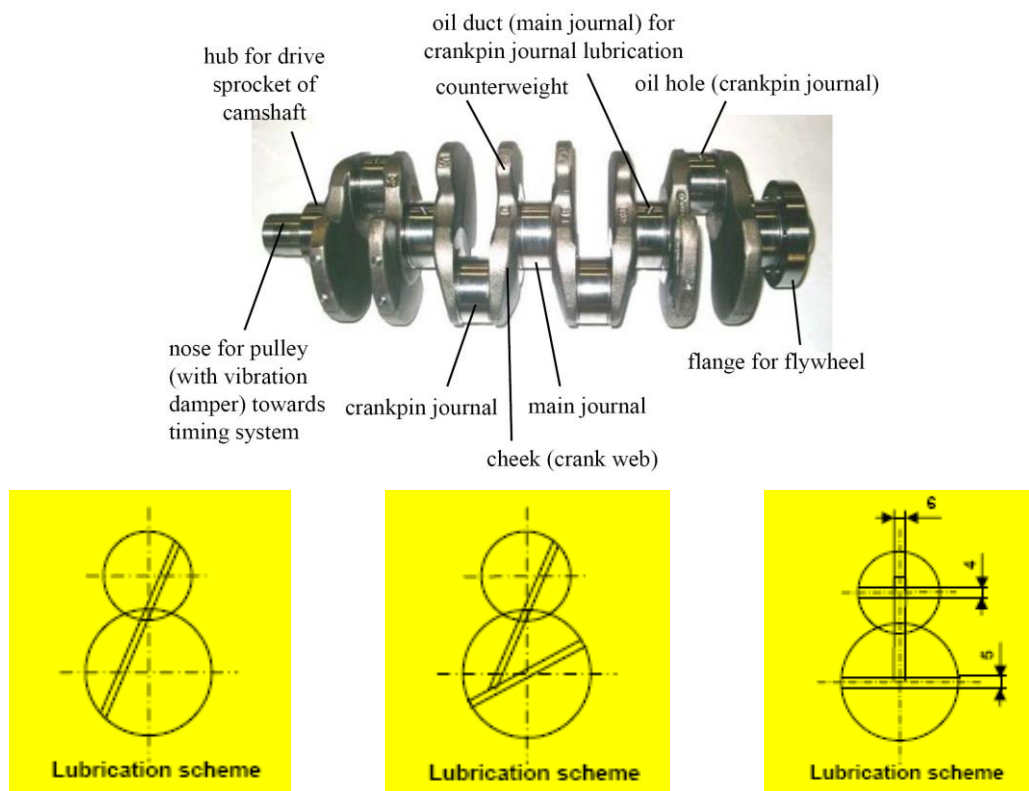
## 4. Crankshaft

The crankshaft is a sequence of cranks (crankpin journal), each crank carrying one connecting rod. Between two main journals there the cheeks. At one end there is the nose for the pulley of the timing system, at the other end there is the flange for the flywheel mounting. Counterweights are commonly added to the cheeks to balance and reduce the load on the main bearing. From the bending perspective, the critical point are **curvature radii on main journals** and **crankpin journals**.

About lubrication, depending on the scheme to feed oil from the main journal to the crankpin journals, there are three different solutions:

- Single diagonal channel very simple, almost correct
  - Double diagonal channels solution adopted for crank journals with lubricant groove only on one half of the bushing
  - Three cross channels abandoned solutions, problems about lubrication oil positioning

In the picture below, each crank has 2 counterweights, but it is also possible to have 1 counterweight for each crank which is a low cost solution.



## Material

The crank material is chosen according to the application:

- Cast iron low-medium stressed engine
  - Steel high stressed engine

To further reduce the rotating masses, the crankshaft can be longitudinally drilled (very expensive).

## Design Guidelines

The scheme of a generic crank is reported below. As a first approximation, the main journal and the crankpin journal diameters are assumed equal:

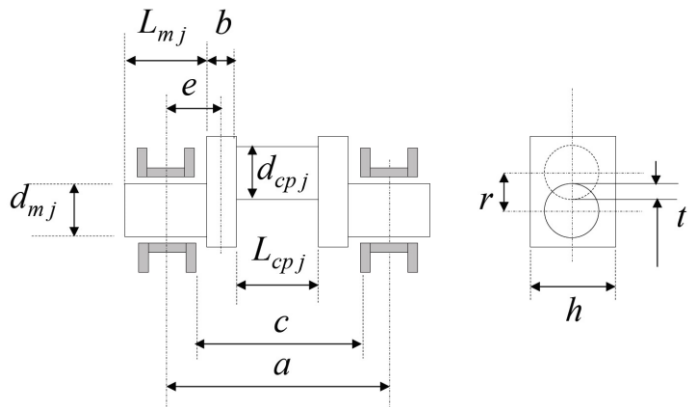
$$d_{mj} = d_{cpj}$$

The crankpin journal diameter  $d_{cpj}$  and the cheek width  $b$  are computed through semi-empirical formulas obtainable from literature.

The crankpin journal length  $L_{cpj}$  and main journal length  $L_{mj}$  are computed taking into account:

- resultant force  $F$  acting along the piston axis
- maximum admissible pressure  $p_{adm}$  on the main bearing (about 18 ÷ 25 MPa)

$$L_{cpj} = \frac{F}{d_{cpj} \cdot p_{ad}}, \quad L_{mj} = \frac{F}{2d_{cpj} \cdot p_{ad}}$$



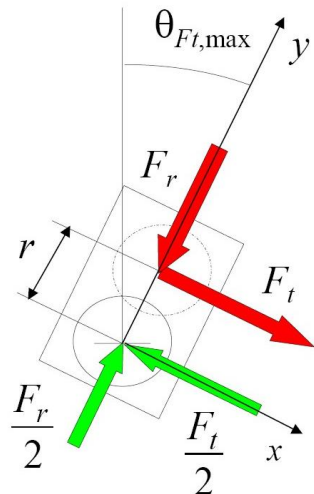
## Structural Verification

The structural verification of the most stressed crank takes into account two different configurations. This because the source of the **tangential effect** on the most stressed crank is different

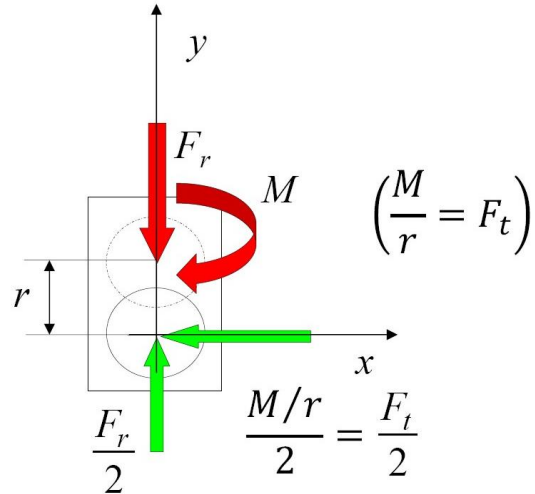
- maximum tangential force  $F_{t,max}$  configuration due to gas pressure,
- TDC configuration, due to torque  $M$  from other cranks.

In both configurations, the equivalent stresses in the crankpin journal, main journal and cheek must be lower than the admissible.

$F_{t,max}$  configuration



TDC configuration



<b><i>F<sub>t,max</sub></i> configuration</b>			
<b>Element</b>	<b>Loads</b>		<b>Stresses</b>
Crankpin Journal	Bending Moment $M_y$	$M_y = \frac{F_t}{2} \frac{a}{2}$	$\sigma_b = \frac{\sqrt{M_x^2 + M_y^2}}{W_b}$
	Bending Moment $M_x$	$M_x = \frac{F_r}{2} \frac{a}{2}$	$\tau = \frac{M_z}{W_t}$
	Torque $M_z$	$M_z = \frac{F_t}{2} r$	$\sigma_{eq} = \sqrt{\sigma_b^2 + 3\tau^2} \leq \sigma_{adm}$
Main Journal	Bending Moment $M_y$	$M_y = \frac{F_t}{2} e$	$\sigma_b = \frac{\sqrt{M_x^2 + M_y^2}}{W_b}$
	Bending Moment $M_x$	$M_x = \frac{F_r}{2} e$	$\tau = \frac{M_z}{W_t}$
	Torque $M_z$	$M_z = \frac{F_t}{2} r$	$\sigma_{eq} = \sqrt{\sigma_b^2 + 3\tau^2} \leq \sigma_{adm}$
Cheek	Normal force $N$	$N = \frac{F_r}{2}$	$\sigma = \frac{N}{A} + \frac{M_x}{W_{bx}} + \frac{M_z}{W_{bz}}$
	Bending Moment $M_x$	$M_x = \frac{F_r}{2} e$	
	Bending Moment $M_z$	$M_z = \frac{F_t}{2} r$	$\sigma_{eq} = \sigma \leq \sigma_{adm}$

<b><i>TDC</i> configuration</b>			
<b>Element</b>	<b>Loads</b>		<b>Stresses</b>
Crankpin Journal	Bending Moment $M_x$	$M_x = \frac{F_r}{2} \frac{a}{2}$	$\sigma_b = \frac{M_x}{W_b}, \quad \tau = \frac{M_z}{W_t}$
	Torque $M_z$	$M_z = \frac{F_t}{2} r$	$\sigma_{eq} = \sqrt{\sigma_b^2 + 3\tau^2} \leq \sigma_{adm}$
Main Journal	Bending Moment $M_x$	$M_y = \frac{F_r}{2} e$	$\sigma_b = \frac{M_x}{W_b}, \quad \tau = \frac{M_z}{W_t}$
	Torque $M_z$	$M_z = \frac{F_t}{2} r$	$\sigma_{eq} = \sqrt{\sigma_b^2 + 3\tau^2} \leq \sigma_{adm}$
Cheek	Normal force $N$	$N = \frac{F_r}{2}$	$\sigma = \frac{N}{A} + \frac{M_x}{W_{bx}} + \frac{M_z}{W_{bz}}$
	Bending Moment $M_x$	$M_x = \frac{F_r}{2} e$	
	Bending Moment $M_z$	$M_z = \frac{F_t}{2} r$	$\sigma_{eq} = \sigma \leq \sigma_{adm}$

## Static Analysis

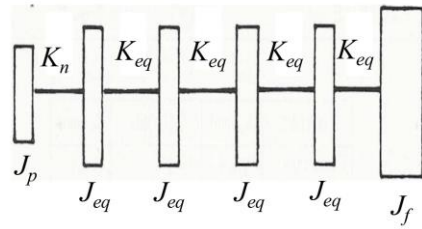
About the static analysis, the crankshaft is modeled as a *standstill beam*, with load defined at a specific time (i.e. specific crank angular position  $\vartheta$ ). The goal of the static analysis is to evaluate the **bending moment acting on each crank** and the relative stresses. The methodology consists of:

1. Compute the gas pressure and inertial forces from the crank-slider mechanism,
2. Compute the forces acting on the main journal
3. Compute the reactions and polar plots (load evolution in the kinematic pair crankshaft-conrod) of the main bearings assuming two different schemes:
  - **Isostatic** crankshaft is considered as the assembly of  $n$  cranks not linked together,
  - **Hyperstatic** crankshaft is considered as a continuous beam on  $n$  supports.
4. Compute the static bending moments acting on each crank
5. Compute the correspondent stresses
6. Static verification comparing Von Mises equivalent stress with that admissible of the material.

## Dynamic Analysis

### 1. Lumped Parameter

Analytically, we can only find torsional bending (90% of the stresses), for all the other stresses one must refer to FEM. To compute the torsional stiffness, it is required to exploit a lumped parameter system torsionally equivalent to the considered crankshaft ( $J$  = inertia,  $K$  = stiffness). Each crank is modeled as a stiff disk with equivalent moment of inertia  $J_{eq}$  and a massless bar with equivalent torsional stiffness  $K_{eq}$ . Note that  $J_p$  stands for pulley inertia, whereas  $J_f$  stands for flywheel inertia.



The methodology consists of:

1. Definition of the equivalent lumped parameter system,
2. Compute the natural frequencies and mode shapes of a free single-cylinder engine.
3. Fourier decomposition of gas torque harmonics that are in resonant condition (Campbell diagram)
4. Identification of engine harmonics which are in resonant condition
5. Shift the analysis to the multicylinder engine
  - Phase diagram of the cranks,
  - Phase diagram of the harmonics,

6. Computations of the forced response under resonant condition and corresponding torsional dynamic stresses (to add to stresses deriving from the static analysis).

Some approximations and assumptions are needed for the dynamic analysis:

- stress intensification at radii between cheek and crankpin is semi-empirical from literature,
- interactions between torsional, bending and axial modes are not considered,
- clearances and lubricant are not considered,
- interaction between crankshaft and cylinder block is not considered,
- constraint effect of the journals is not considered.

To study the dynamic behavior of the system, one must solve the **equation of motion** (free behavior + forced response):

$$[J]\{\ddot{\Phi}\} + [K]\{\Phi\} = \{M(\vartheta)\}$$

where:

- $[J]$  Diagonal inertia matrix  $v \times v$ ,
- $\{\Phi\}$  Torsional dof,
- $[K]$  Tridiagonal symmetric stiffness matrix  $v \times v$ ,
- $\{M(\vartheta)\}$  Engine torque,
- $v$  Number of torsional dof,  $v = \# \text{cylinders} + 2$  (flywheel and pulley)

The inertia matrix  $[J]$  has constant coefficients over time. The equivalent moment of inertia  $J_{eq}$  is considered average on the engine cycle and constant in time. The equivalent stiffness  $K_{eq}$  of a torsional bar is instead computed semi-empirical through literature: Carter, Tuplin, Timoshenko, Zimanenko, etc.

## 2. Free response

The free response of the unloaded system is:

$$[J]\{\ddot{\Phi}\} + [K]\{\Phi\} = 0$$

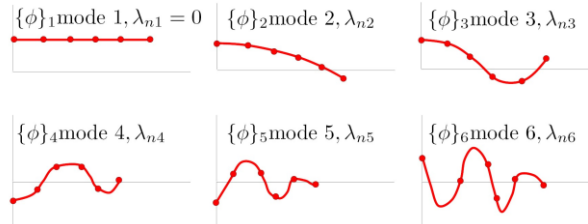
Torsional natural frequencies (eigenvalues) and corresponding vibration modes (eigenvectors) are solved by:

$$\{\Phi\} = \{\Phi_0\} e^{i\lambda_n t} \implies \det(-\lambda_n^2 [J] + [K]) = 0$$

where:

- $\lambda_{ni}$  i-th torsional natural frequency ( $i = 1$  represents  $v$  with  $\lambda_{n1} = 0$  rigid mode),
- $\{\Phi\}_i$  i-th torsional mode,

Since  $J_{eq}$  coefficients are constant over time, then the natural frequencies are constant and independent both from crank angle  $\vartheta$  and the engine speed  $\omega$ . Consequently, these natural frequencies are represented by horizontal lines in the Campbell diagram ( $\lambda$  vs  $\omega$ ).



### 3. Harmonic Analysis of Engine Torque

To study forced response of the system, one must face the harmonic analysis of the engine torque (gas + inertia). Indeed, the engine torque generated by gas pressure and inertia forces can be developed in a Fourier series as sum of harmonics:

$$M(\vartheta) = M_g(\vartheta) + M_a(\vartheta)$$

where:

- Engine gas term  $M_g(\vartheta) = p_g(\vartheta) \frac{\pi D^2}{4} \cdot f_1(\vartheta) \cdot r$  20 harmonics are sufficient
- Inertia term  $M_a(\vartheta) = -m_a \omega^2 r \cdot 2(\vartheta) \cdot r$  8 harmonics are sufficient

In the gas term development, we have a static contribution  $A_0$  which provides power but does not cause torsional oscillation, whereas all other terms only cause torsional oscillation of the crankshaft.

In the same way, in the inertia term development, it is possible to recognize the terms that cause torsional oscillation of the crankshaft.

The Fourier series of the overall engines considers the combination of vectors that represents the harmonics of the gas and inertial reciprocating forces. Each vector has amplitude and phase for the k-th harmonic.

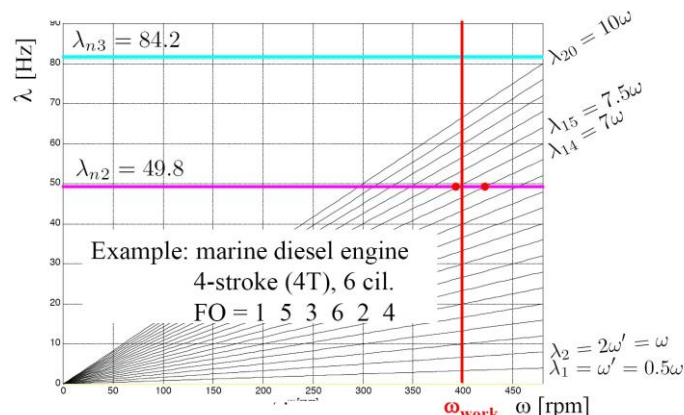
### 4. Resonant Harmonics

The resonance of one of the natural mode of the crankshaft is the result of the interaction between:

- engine torque harmonics,  $\lambda_{ni}$  Eigenvalues of the free response
- crankshaft natural frequencies.  $\lambda_k = k \cdot \omega'$ ,  $k = 1 \dots 20$ ,  $\omega' = \frac{\omega}{2}$  for 4T engine

To identify the harmonics of the engine torque that are resonant, use the Campbell diagram ( $\lambda$  vs  $\omega$ ). Since torsional natural frequencies are a straight line, but the pulsation of the generic engine torque do not (they are time dependent), then, for a specific engine speed  $\omega_{work}$ , the resonant harmonics are those near the intersection between the crankshaft natural frequencies and the vertical line of  $\omega_{work}$ . To sum up:

- horizontal line crankshaft natural frequencies  $\lambda_{ni}$  time-independent
- oblique line engine torque harmonics  $\lambda_k$  time dependent
- vertical line engine working speed  $\omega_{work}$

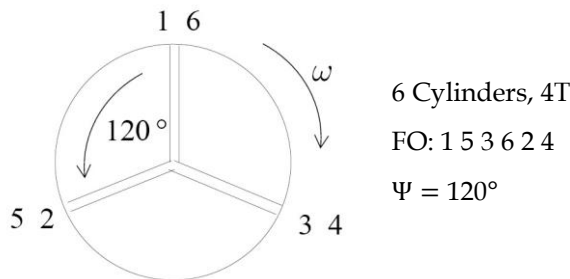


## 5. Multi-cylinder engine

In the analysis of the multi-cylinder engine, it is required to introduce the **phase shift**  $\delta_{k,j}$  (k-th harmonics of the j-th cylinder) between the engine torque harmonics. To identify the phase shift  $\delta_{k,j}$  between the harmonics, it is required to refer to the phase (stellar) diagrams. In a multicylinder engine the angular phase shift is indicated by  $\Psi$ :

$$\Psi = \begin{cases} \frac{4\pi}{z} & \text{for 4T engine} \\ \frac{2\pi}{z} & \text{for 2T engine} \end{cases}, \quad z = \# \text{cylinders}$$

By knowing the Firing Order and the angular phase shift, then one can draw the phase (stellar) diagram of cranks.



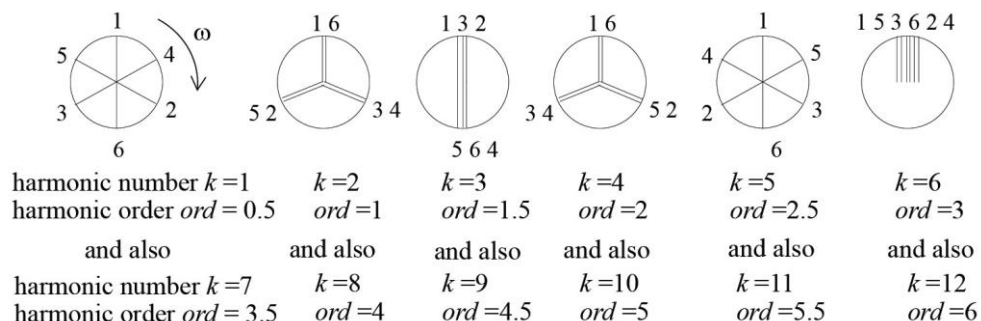
After, the phase shift between the harmonics  $\delta_{k,j}$  is then computed as the product between the

<ul style="list-style-type: none"> <li>• Harmonic order</li> <li>• Angle between cranks</li> </ul>	$ord = \begin{cases} \frac{k}{2} & \text{for 4T engine} \\ k & \text{for 2T engine} \end{cases}$	$\left. \delta_{k,j} = ord \cdot \Psi = \begin{cases} \frac{k}{2}\Psi & \text{for 4T engine} \\ k\Psi & \text{for 2T engine} \end{cases} \right\}$
--	--	--

Finally, with the phase shifts of the harmonics, it is possible to draw the stellar diagram of the harmonics (which is different from the previous that was the stellar diagram of the cranks).

When the harmonics order is a multiple integer of  $z/2$ , all the vectors have same direction. The corresponding engine orders are called **major order** and the relative harmonics are dangerous for NVH. The forced dynamic response (to evaluate torsional stress level) then must be computed for:

- resonant harmonics of the engine torque (Campbell Diagram, point 4 of the analysis),
- resonant harmonics related to major orders.



## 6. Forced Response

In resonant condition, it can be assumed that the forced response amplitude is proportional to the system resonant mode:

$$\{\Phi\}_k = \alpha_k \{\Phi\}_{resonant}$$

where  $\alpha_k$  is a proportionality factor which consider a viscous damping equivalent to the actual damping of the crankshaft.

For each of the dangerous harmonics, the output of this analysis is the **total shear stress**  $\tau_s$  acting on each crank.

$$\tau_s = \tau_{stat,s} + \tau_{dyn,s}$$

## Dynamic Numerical Analysis (FEA-MBA)

Through the Finite Element Analysis (FEA) it is possible to:

- consider actual geometry, loads and forces,
- verify the coupling between modes.

The cylinder block is considered a rigid or deformable body, the constraints between crankshaft and cylinder block are modeled as spring and finally the conrods and pistons are modelled as concentrated mass that contributes to the force acting on the main journals.

However, FEA does not allow to simulate the behavior of the crankshaft that is interfering with others component of the powertrain. Also, gyroscopic effect is neglected, and inertial forces are stationary load.

To obtain a more detail of the behavior, is it required to perform a MultiBody Analysis (MBA) in order to:

- compute and apply inertial forces,
- consider the variability of the moment of inertia,
- consider the hydro-dynamic interaction with the oil (regulated by Reynolds equation),
- consider the local gyroscopic effect.

The simulation results are obtained in terms of displacements, angular velocities and angular accelerations (of the condensed nodes, i.e. master dofs), forces and moments on the nodes required at the MB model set up.

## Waterfall Diagram (3D) and Order Chart (2D)

The Waterfall Diagram and the Order Chart can be obtained by post-processing the MB simulation results:

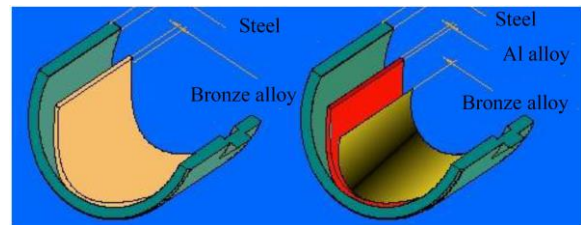
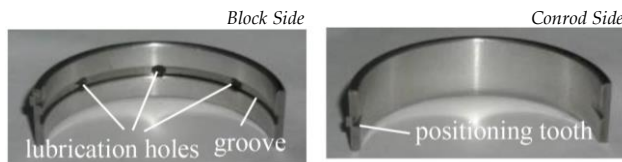
- |                     |    |                            |
|---------------------|----|----------------------------|
| • Waterfall Diagram | 3D | Magnitude vs Frequency,    |
| • Order Chart       | 2D | Magnitude vs Engine Speed, |

These diagrams represent the “dynamic identity card” of the crankshaft and they are useful to identify its critical regimes and because , the crankshaft responds to the external loads in different way depending on the operating condition, then regimes it is necessary to verify the stress state of the crankshaft in order to evaluate its most critical condition.

## 5. Bearings

Crankshaft journals rotate on two half-shells (bushing or bearings) inserted into the main caps and walls of the cylinder block, and into the big eye of the conrods. Each half-shell is composed of structural steel layer and by one or two additional layers (bi-metallic or tri-metallic solution) of anti-friction material (bronze alloy). The purpose of the bearings are:

- support the load generated by the crank mechanism transmitted to the oil film,
- guarantee wear resistance
- absorb geometrical inaccuracies of the journals



Usually one of the two half-shells has a **groove** to collect the oil coming from the channels needed to continuously feed the crankshaft and the conrod. If the crank is heavily stressed (diesel engine), then the central groove is eliminated in favor of a diagonal drilling solution.

The crankshaft is also provided with a thrust bearing to counteract axial loads and the clutch axial force.

Also, a **tapered side** is present in the contact area of the two half-shells to prevent damages to the bushing material (compression force tends to deform the tapered ends).

### Classical Analysis

The force that loads the bearings comes from the crank-slider mechanism:

$$F_H = F_\omega \sin \vartheta, \quad F_V = F_a - F_\omega \cos \vartheta, \quad M_e = Fr \left( \sin \vartheta + \frac{\lambda}{2} \sin 2\vartheta \right)$$

Since these forces are time-dependent (depends on crank angle  $\vartheta$ ), then the bearing reaction is also time-varying leading to dangerous vibrations.

It is then crucial to get **polar plots** of these reactions to analyze the criticalities: in the analysis the crankshaft is considered both *isostatic* and *hyperstatic* to embrace all kinds of solution that is:

- the total reaction is the sum of vectorial reaction for each crank
- the total reaction comes from hyperstatic problem solutions.

Since the coupling between main journal and cylinder block, and between crankshaft crankpin journal and big eye of the conrod is by means of oil film, then the analytical solution is provided by the **Reynolds Equation** which is based on the following assumptions:

- no misalignment between bearing and journal,
- loads on journal constant in magnitude and direction,
- crankshaft, cylinder block and conrod as rigid bodies,
- constant oil viscosity.

The main parameters are:

- Radial clearance  $\delta = R - r$  Difference between journal/bearing radii
- Eccentricity  $e = \overline{O_2 O_1}$  Difference between journal/bearing centers
- Oil thickness  $h(\alpha)$  Maximum oil thickness is  $h_{max}$
- Angular coordinate  $\alpha$  Ranges in the maximum oil thickness region

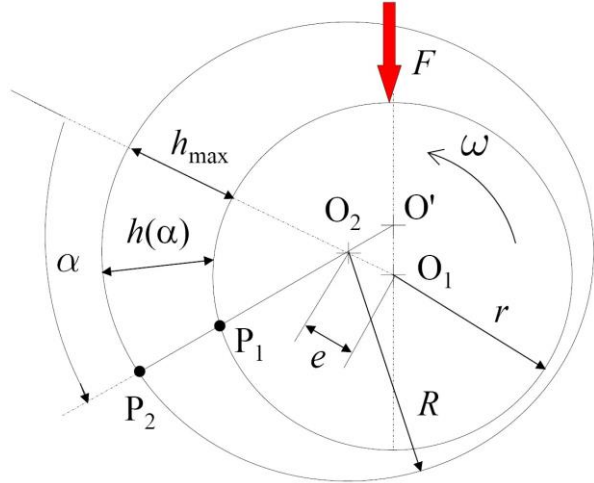
According to the geometry, the oil thickness can be written as:

$$h(\alpha) = \delta(1 + \varepsilon \cos \alpha)$$

where  $\varepsilon$  is the ratio between the eccentricity  $e$  and the radial clearance  $\delta$ .

The solution of the hydrodynamic problem (in terms of pressure  $p$ ) is given by the **Reynolds Equation**:

$$\frac{dp}{d\alpha} = \frac{6R\mu v}{h^2(\alpha)} \left[ 1 - \frac{2q}{vh(\alpha)} \right]$$



where:

- $p$  Oil film pressure
- $q$  Oil flow rate
- $\mu$  Oil dynamic viscosity
- $v$  Relative velocity between the lubricated surfaces (journal and bearing)
- $R$  Bearing radius

Note that the analytical solution of the Reynolds Equation is possible only if no pressure is considered at the point of maximum oil thickness:  $p(h_{max}) = 0$ . Other supplementary parameters to describe the bearing behavior are:

- Sommerfeld number  $S$
- Bearing axial length  $B$
- Elongation  $B/(2R)$  Useful to identify the *load capacity*
- Friction coefficient  $f_c = M/FR$  Depends on  $\mu$ ,  $p_s$  and  $\omega$
- Characteristic pressure  $p_s = F/(2BR)$
- Adimensional flow rate  $q = 2Q/(\omega B \delta R)$

By solving the Reynolds Equation, we obtain the **maximum pressure  $p_{max}$**  and the **minimum oil thickness  $h_0$  at temperature  $T$** ; as function of the diametral clearance  $g = 2\delta$  or of the elongation. Low value of the elongation leads to oil leakages, but too high value of the elongation may cause misalignment between bearing and journal.

Note that by increasing the load  $F$  or decreasing the engine speed, the oil film thickness decreases. The minimum oil thickness must be at least to the sum of the peak-valley roughness of the coupled surfaces (journal-bearing).

## Numerical Coupled FEA-MBA

Since the Reynold Equation provides solutions for infinitely short/long bearing, the FEA-MBA analysis gives back the solution for the actual configuration of the bearing. Numerical simulations consider:

- actual length of the bearing,
- time-dependent forces,
- misalignment,
- elasticity of the components.

The verifications for the MB model validation uses the same criteria of the MB of the crankshaft:

- correctness of the Firing Order (FO),
- cyclic trend of the flywheel angular velocity,
- correct trend of the radial forces on the main bearing.

The target of the MB model is to provide the **crankshaft dynamic behavior** and the corresponding **dynamic response of the bearings**. Starting from the FE model and then the MB model, one obtains:

- elasto-hydrodynamic solution,
- 3D distribution of oil film pressure and thickness,
- oil flow rate computation.

Different model complexity may be adopted in the investigation:

<b>CR</b>	- Rigid main Journal - No misalignment - No crankshaft dynamics	All rigid components, no FE model are required
<b>CE</b>	- Rigid main Journal and elastic bearing - No misalignment - No crankshaft dynamics	FE model of single wall and cap
<b>BR</b>	- Elastic crankshaft and rigid cylinder block - Yes misalignment - Yes crankshaft dynamics	FE model of crankshaft
<b>BE</b>	- Elastic crankshaft and rigid cylinder block - Yes misalignment - Yes crankshaft dynamics - Yes Cylinder Block dynamics	FE model of crankshaft and cylinder block



## 6. Piston

The main purposes of the piston are:

- transfer gas pressure to the conrod,
- discharge of exhaust gases,
- support the small eye of the conrod,
- provide good sealing to avoid blowby,
- reduce friction.

The **piston top** is shaped to optimize the combustion chamber (the **bowl** in diesel engines) and valve seats are directly machined on the top. The **skirts** works as a guide for the reciprocating motion and contributes for the 25% to the heat flow between piston and liner. The inner part of the piston may present a cooling gallery to cool down the interior. In case of high stressed engine, bronze bushings are inserted in the hubs.



**Piston rings** ensure tightness of the combustion chamber avoiding the blow-by phenomenon of the gas. They also control oil amount that lubricates the liner surface that is in contact with the piston. In general, three rings are adopted:

- |   |   |
|---|---|
| • 1 <sup>st</sup> ring,                     | sealing ring to avoid blow-by,            |
| • 2 <sup>nd</sup> and 3 <sup>rd</sup> ring, | oil scraper rings to control lubrication. |



## Material

The material for pistons must have high mechanical strength, high heat resistance and low thermal expansion. Passenger engine pistons are made of:

- |                       |                  |                     |
|-----------------------|------------------|---------------------|
| • Al alloys           | AlSiMg, AlCuMgSi | gasoline engines,   |
| • Eutectic Al alloys, | AlSi12, AlSi10   | diesel engines,     |
| • Cast iron           |                  | industrial engines. |

On the contrary, piston rings are made of cast irons with Cr-plating and Mo-plating to increase resistance to wear and high temperatures.

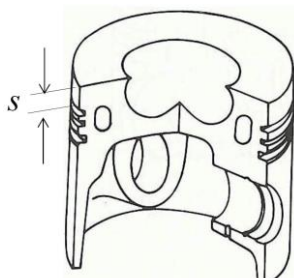
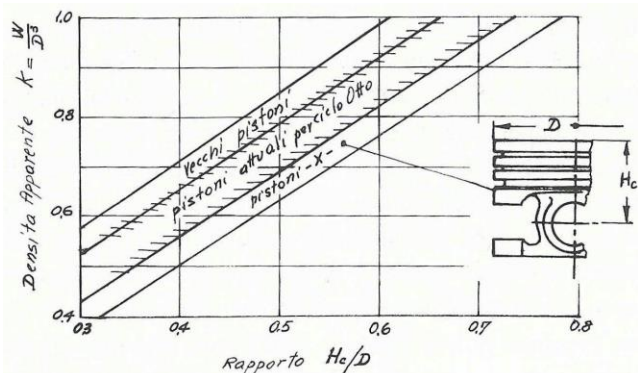
Production technologies are die cast (economic but low mechanical resistance) and metal forming (expensive but high mechanical resistance). To avoid crack propagation, the surface finishing are grinding and diamond machining. Also, an alumina coat is performed on the top to increase the adiabatic condition of the bowl.

## Design Guidelines

### Piston

Starting from the bore  $D$  and the target (estimated) weight  $W$ , one can find the **apparent density  $K$** , and consequently the geometrical ratio  $r_p$  which is the **compression height  $H_c$**  over the bore. Thus,  $H_c$  is obtained.

$$K = \frac{W}{D^3} \Rightarrow H_c$$



Considering the top pf the piston as a circular plate, one compute the thickness  $s$  of the piston to according to the literature formula (verified by FEA):

$$s = \frac{D}{2} \sqrt{\frac{p_{max}}{\sigma_{adm}}}$$

Alternatively, one can enter suitable tables. Note that the top thickness  $s$  highly influences the bowl shape in diesel engines, thus it is required to perform kinematic simulation about the valve interference at TDC.

With these geometrical values, one must verify that the compressive stress on the top is lower than the admissible stress:

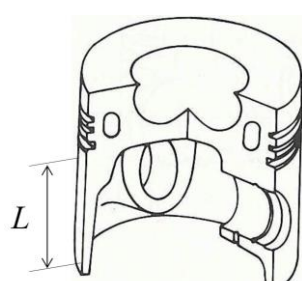
$$\sigma_c = \frac{p_{max} D^2}{D_c^2 - D_i^2} \Rightarrow \sigma_c \leq \sigma_{adm}$$

where:

- $D_c$  groove diameter (diameter of the bowl),
- $D_i$  piston inner diameter,

Piston material	Allowable pressure $p_{adm}$ [MPa]
Al alloy	0.98
Cast iron	0.44 – 0.64

Finally, the length of the skirt  $L$  is limited by the normal force depending on the material as shown in the table aside.



Therefore, basing on the value of the admissible pressure, the length of the skirt can be computed as:

$$p_{adm} = \frac{F_{n,max}}{L \cdot D} \Rightarrow L = \frac{F_{n,max}}{p_{adm} \cdot D}$$

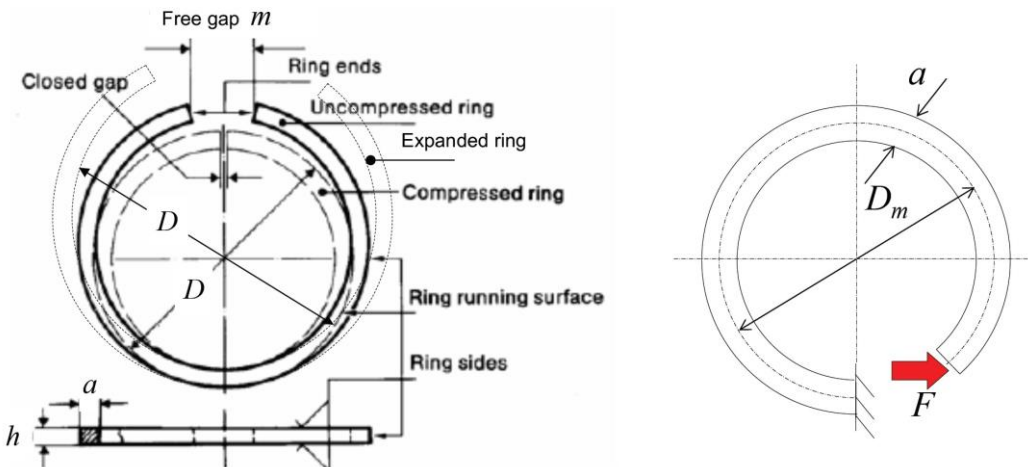
However, as a first attempt to define the length  $L$ , one can consider a uniform pressure distribution, as the pin axis should be half of the piston compression  $H_c$ , then:

$$L = 2 \cdot H_c$$

## Piston ring

About piston rings, all forces acting on the ring must be considered together with radial and tangential load distributions. During mounting, the ring must be expanded since it must pass through the top of the piston crown. In this condition the inner ring diameter is assumed to be equal to the bore  $D$ . Starting from this assumption, a preliminary dimension of the piston ring follows the below table:

Radial wall thickness $a$	$0.029D - 0.033D$
Axial width $h$	$0.1a - 0.6a$
Free gap $m$ (uncompressed ring)	$0.08D - 0.12D$



The piston ring is then modeled as a curved beam loaded by a concentrated force  $F$  which is function of the maximum admissible pressure:

$$F = \frac{P_{adm} D_m h}{2}$$

Once the value of the force  $F$  is obtained, it is required to compute the radial displacement  $u$  and the maximum bending stress  $\sigma_b$  in the ring:

- $u$  radial displacement  $u = \frac{3\pi FD_m^3}{8EI} \approx 8a$
- $\sigma_b$  bending moment  $\sigma_b = \frac{FD_m a}{2I} \Rightarrow \sigma_b \leq \sigma_{adm}$

Through the radial displacement, it is required to compute two additional stresses related to the mounting procedures, the expansion for the fitting in the groove and the compression for the mounting in the liner:

- $\sigma'$  stress due to reduction of the ring diameter to working value (bore)
- $\sigma''$  stress related to opening displacement

$$\sigma' = \frac{E}{\frac{3\pi}{4}\left(\frac{D_m}{a} - 1\right)^2 a} m, \quad \sigma'' = \frac{E}{\frac{3\pi}{4}\left(\frac{D_m}{a} - 1\right)^2 a} \frac{(8a - m)}{a}$$

The static ring verification requires that  $\max(\sigma', \sigma'') \leq \sigma_{adm}$ .

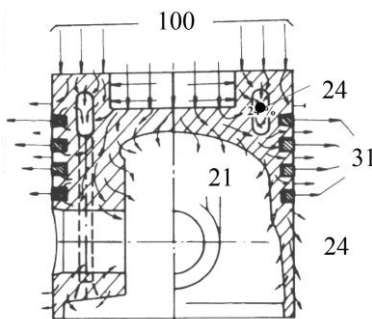
## Numerical Analysis

About piston group, the **thermal behavior** is crucial because the thermal field acting on the piston deforms more the hub zone than the lower part of the piston.

To ensure a good fitting between the piston and the liner, the design of the lower part of the piston must take into account this thermal deformation of the piston skirt (usually different materials are used for top and bottom of the engine, and also barrel shape are exploited for counteracting the thermal expansion).

Just one part (25-30%) of the fuel thermal capacity is transformed into mechanical power because another important amount (about 40%) goes to stress the piston and the liner. The heat is transferred:

- convection to the cooling fluid,
- conduction to the body of the piston,
- radiation to the top op the piston in the combustion chamber.



Considering all the thermal power exchanged (40% of the overall) the subdivision with the other part is:

- 24% to the cooling gallery,
- 31% to the liner through the rings
- 21% to the piston hub,
- 24% to the skirt

In thermal analysis the convection coefficient and the heat transfer coefficient are function of the swirl and squish motion, therefore very complicated to compute! To target of numerical analysis is to get temperature map and heat transfer coefficient in various points of the piston.

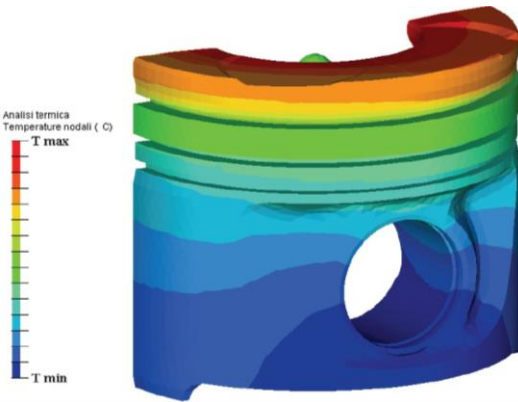
	STATIC	THERMAL	THERMO-STRUCTURAL
Property	MAT01	MAT04	MAT01 + MAT04
Mesh	3D Tetra – 2D Tria	3D Tetra – 2D Tria	3D Tetra – 2D Tria
Constraints	Pin with RBE2 Ring with RBE3 Virtual Spring for ring/liner Contact surface piston/pin	Convective surfaces Nodal Temperatures Top - 180 °C Skirts - 120 °C Interior - 100 °C	Piston hub with RBE2 Temperature
Loads	Gas pressure (compression)	Thermal Flux	Output Thermal + Static

The load condition to be taken into account in the post-processing are **temperature field**, **pressure in the bowl** and **inertial forces**. These loads are studied individually and then superimposed to evaluate the stress state.

## Piston Static Thermal Analysis

The initial condition for the static thermal analysis is represented by the imposed heat flux from the combustion. This heat flux is imposed only on the exchanges surfaces that is the piston top.

Then, assign the thermal coefficient from the numerical analysis, or literature, and calibrate them through iterative procedure.



Provided the material characteristics and the correct mesh, verify that all the power entering the piston is equal to the heat power outgoing the piston external surfaces.

The result of the static thermal analysis are:

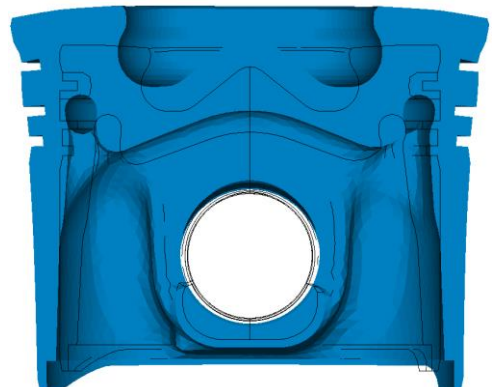
- thermal unbalance between the sides of the piston,
- isothermal zones,
- thermal gradient,
- nodal thermal analysis

## Piston Thermo-Structural Analysis

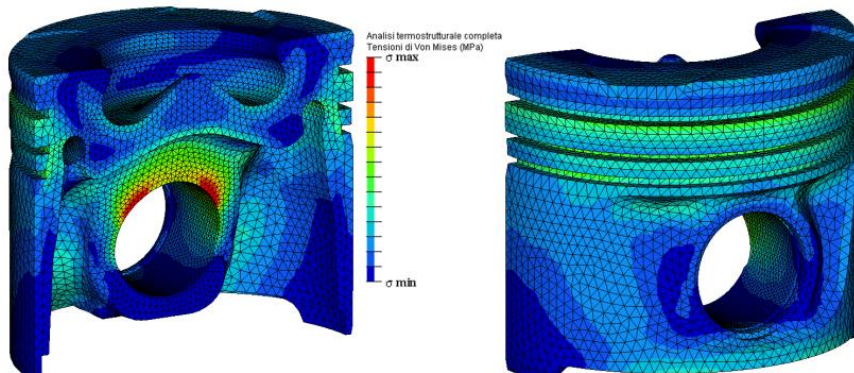
In the thermo-structural analysis, the loads are the thermal load computed by the static thermal analysis and the mechanical load ( $p_{max}$  at the beginning of the expansion). On the contrary, the boundary conditions are the nodal temperatures resulting from the static thermal analysis, and the material properties.

The considered load cases are:

- Temperature field,
- Pressure in the bowl,
- Inertial forces.



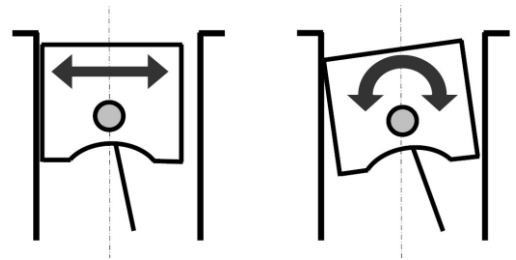
The result of each load is superimposed to evaluate the overall stress state. The result in terms of thermal and mechanical deformation (deformation due to thermal field and due to inertial forces) provide the guide for the choice of the design phase of the piston. Finally, this analysis provides results in terms of strain and stresses.



## Piston Slap

Although the reduced gap between piston and liner, the piston can still move in the liner, because the thrust force  $F_n$  change in sign several times during the cycle. The movements of the piston then result:

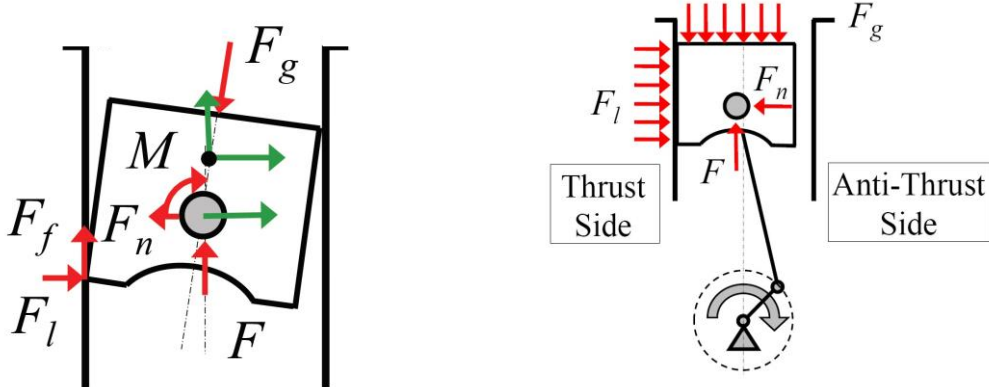
- translation perpendicular to cylinder axis,
- rotation around pin axis (tilting),



These movements are named piston slap movements which cause noise and wear, especially in diesel engines.

The study of the piston slap is based on the free body diagram. The simplified and full free body diagram allows to write the equation of motion and evaluate the forces in every time instant. However it is not sufficient to compute the energy dissipated during the impact piston-liner. The forces acting during the slap are:

- $F_g$  gas force,
  - $F_n$  thrust force exerted by the conrod through the pin,
  - $F_l$  reaction force of the liner,
  - $F_f$  friction force
  - $M$  torque due to the piston-pin contact
- $$F_f = \mu_c \cdot F_l$$
- $$M = \mu_s d_s / 2 \sqrt{F_n^2 + F^2}$$



## Piston Slap Effect

The piston slap effects are relevant in particular in diesel engines due to the high pressure combustion pressure. The effects of the piston slap phenomenon are:

- emission of sound waves,
- cavitation of the coolant fluid,
- sub-superficial fatigue, repeated impacts cause Hertzian fatigue leading to internal cracks.

Note that the crankcase is the main component that transmit engine noise through vibrations (about 30%). Critical conditions are at idle and low spins speed and the maximum peak is obtained at cranking.

Also, high pressure wave can cause cavitation of the coolant fluid (localized boiling).

## Methods to decrease Slap Effect

Three different methods can be adopted to decease piston slap:

- piston offset,
- piston offset + vertical shift of the piston center of gravity,
- increase the number of oil scraper ring.

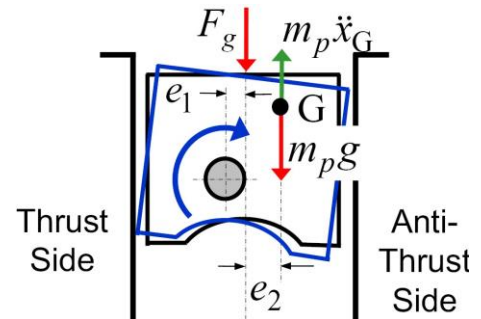
### Piston Offset

The pin axis is moved towards the major thrust side by a quantity  $e_1$ , consequently the piston center of gravity shifts towards the minor thrust side by a quantity  $e_2$ .

The moment  $M_0$  causes a rotation of the piston relaxing the impact on the major thrust force (higher dissipation of the kinetic energy).

$$M_0 = F_g e_1 + (g - \ddot{x}_G) m_p (e_1 + e_2)$$

Best benefits are obtained for  $e_1 \leq 0.125D$  (12% of the bore).

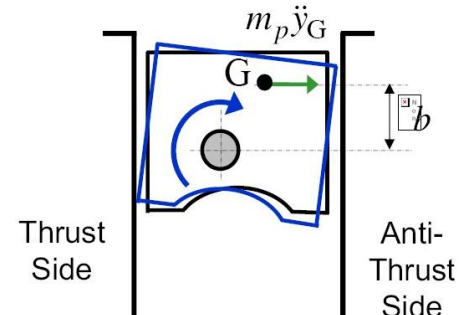


### Piston Offset + vertical shift of the piston center of gravity

The centre of gravity of the piston is moved upwards along the vertical axis by the quantity  $b$  with respect the pin axis.

The lateral inertial force changes its arm and the moment  $M_y$  causes a further rotation of the piston and favors a specific impact configuration.

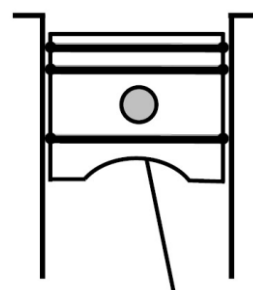
$$M_y = m_p \ddot{y}_G \cdot b$$



### Additional Oil Scraper ring

The additional oil scraper ring are positioned at the bottom of the piston skirt. The main advantages are:

- damping and lift effect of the oil film,
- decrease of impact force between piston and liner,
- better hydrodynamic lubrication.



However, the disadvantages are Three different methods can be adopted to decease piston slap:

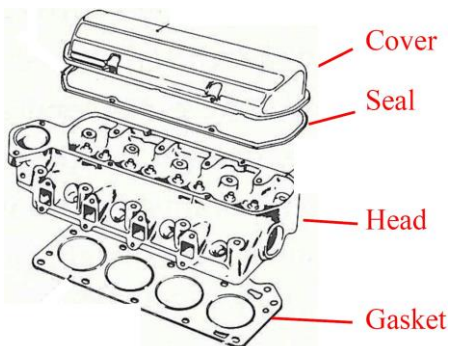
- higher power friction,
- increase of piston mass and so inertial forces



## 7. Cylinder Head

The main purposes of the cylinder head are:

- hosts intake and exhaust ports,
  - control the mechanism of the valve,
  - support the component for combustion (injection and sparking),
  - supply pipes and volumes for oil and coolant circulation,
  - define the shape of the combustion chamber together with the head of the piston.

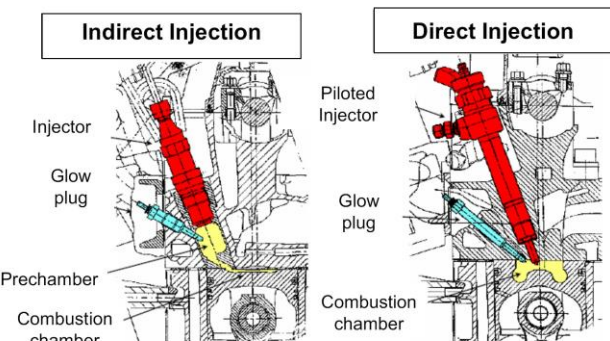


The cylinder head structure is mainly constituted by two plates connected together along their outer edge in a prismatic solid.

The cylinder head is connected to the engine block by studs or screws whose position determine the mechanical stresses.

The sealing with the block is guaranteed by the gasket which avoids the passage of exhaust gases from the combustion chamber to lubricant circuits.

For stiffness reason, the integral solution (cam carrier + cylinder head) is preferable, however, for mounting reason usually the head is split in two different parts. In diesel engines, the cylinder head geometry is defined by the combustion type: indirect (mainly industrial engines) and direct injection (passenger cars).



The positioning of the intake and exhaust port is driven by the following criteria:

Exhaust manifold in front of driving side	Intake manifold in front of driving side
<ul style="list-style-type: none"> <li>- Better temperature control on manifold and turbo</li> <li>- Better fuel protection in case of frontal bump</li> <li>- Possibility to have flexible point to damp down vibration</li> </ul>	<ul style="list-style-type: none"> <li>- Close-coupled catalyst with large dimensions</li> <li>- lower light-off time of the catalyst (no wind)</li> <li>- Simpler exhaust pipe design</li> <li>- Simpler and stiffer oil pan (no interference with exhaust)</li> </ul>

## Material

Usually, the cylinder head is obtained:

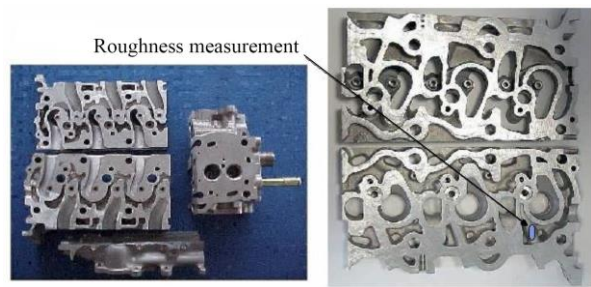


AlSi7, AlSi9,

## Cooling

The cooling circuit into the cylinder head must avoid dangerous overheating especially between the housing of the valves. For this purpose, the design of the cooling path is mainly defined through CFS numerical analysis.

Good results are achieved when the coolant flows near hot surfaces at specific adequate speeds. A uniform working condition of the cylinder head is obtained if the temperature is maintained almost constant.

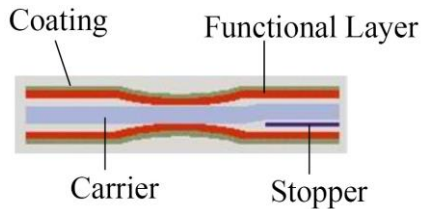


To allow proper cooling, the roughness of the internal surfaces (critical zone) must be in the range of  $2 \div 4 \mu\text{m}$ .

## Gasket

The gasket must seal the head from the block. It has to resist to high temperature, high pressure and corrosion by gas, water and lubricant. The most common solution is a multi-layer metal sheet with proper metal forming for increase stiffness property.

The external layer is made of harmonic steel, whereas the internal layers (carriers) are made by common or laminated steel to improve structural stiffness and supply the correct value of general thickness. Finally an external rubber coating cover the whole gasket. Also, the gasket is provided of stoppers in the most stressed points (maximum pressure of compression).



To verify the sealing capability, it is required to perform numerical FE simulation (Fuji film test).

## Cover

The head cover is needed to close the cylinder head but it can also be functional for:

- splitting volume between lubricant and blow-by gas,
- sealing of part of the intake ports,
- define the capacity of the air filter.

Usually it is made by:

- |            |                                      |
|------------|--------------------------------------|
| • Steel    | cheap solution, potentially noisy    |
| • Al-alloy | stiffer solution, potentially noisy  |
| • Plastic  | cheap and quiet solution, less stiff |
| • Mg-alloy | light and quiet solution, expensive  |



To avoid that engine vibrations are transmitted up to the head, rubber rings are usually exploited in between the screws and the head.

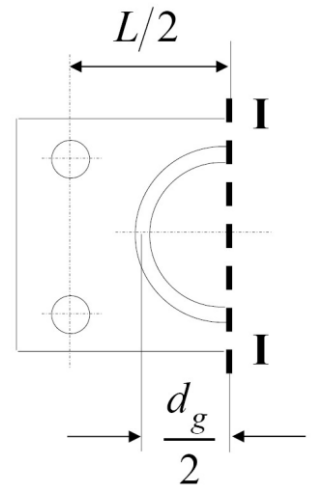
## Design Guidelines

The first attempt considers only half cylinder head. The initial loading condition is only provided by the pre-load of the fixing screw (or studs). The gasket sealing force is given by:

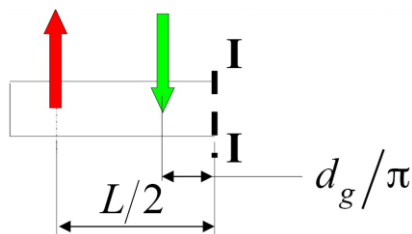
$$F^* = p_{max} \frac{\pi d_g^2}{4}$$

in which  $d_g$  is the mean diameter of the cylinder head gasket.

The screws (or studs) fixing pre-load is taken into account multiplying the force  $F^*$  by  $(1 + k)$  where  $k$  coefficient is commonly assumed equal to 0,5.

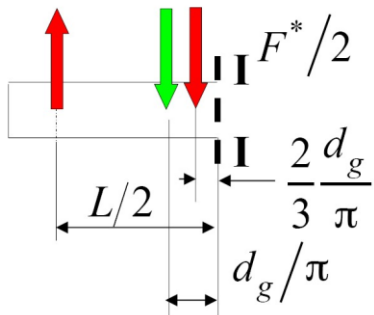


In assembly (static) condition, the gasket reacts to the input force (fixing pre-load) with a reaction located at the center of mass located at  $d_g/\pi$  from the central cross section. According to these forces, the bending moment and stress:



$$M_{b,st} = \frac{F^*(1+k)}{2} \cdot \frac{L}{2} - \frac{F^*(1+k)}{2} \cdot \frac{d_g}{\pi} \Rightarrow \sigma'_{b,st} = \frac{M_{b,st}}{W_{I-I}}$$

However, in operating (working) condition, one must also consider the gas force which acts in the center of mass at a distance  $2d_g/3\pi$  from the central cross section. Certainly, this additional force increases the reaction force of the gasket. Thus, the bending moment and stress in working condition are:



$$M_{b,dyn} = \frac{F^*(1+k)}{2} \cdot \frac{L}{2} - \frac{kF^*}{2} \cdot \frac{d_g}{\pi} - \frac{F^*}{2} \cdot \frac{2d_g}{3\pi} \Rightarrow \sigma'_{b,dyn} = \frac{M_{b,dyn}}{W_{I-I}}$$

Since the cylinder head is in contact with the gas exhaust, then also a temperature gradient is present leading to a further thermal stress  $\sigma_T$ . In conclusion, the final verification in working condition is such that:

$$\sigma_T = \frac{E\alpha\Delta T}{2(1-\nu)} \Rightarrow \sigma'_{b,dyn} + \sigma_T \leq \sigma_{adm}$$

## Screw Design

The first critical parameter is the assembly pre-load  $F_{v,lim}$ . Considering the parameter  $i$  as the number of screws or stud used for each cylinder, then one obtains:

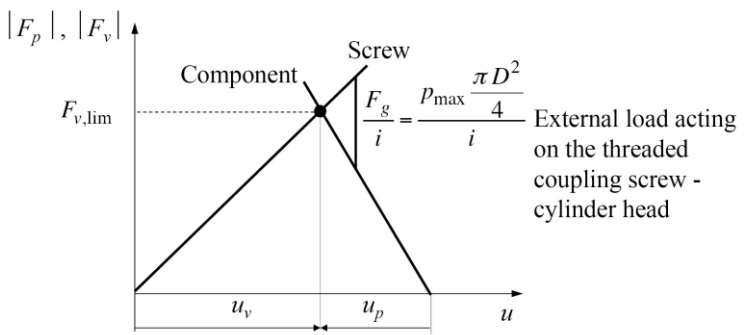
$$F_{v,lim} = \frac{F^*(1+k)}{i}$$

By knowing the deformability of the screw  $\delta_v$  and that of the cylinder head  $\delta_p$ , one can compute the axial displacement of the screw (extension) and that of the component (compression). The interference diagram is obtained as reported below.

In the diagram all possible interference losses must be taken into account:

- fixing uncertainty
- slack
- possible thermal expansion

Finally, one must perform static and fatigue verification of the screw.



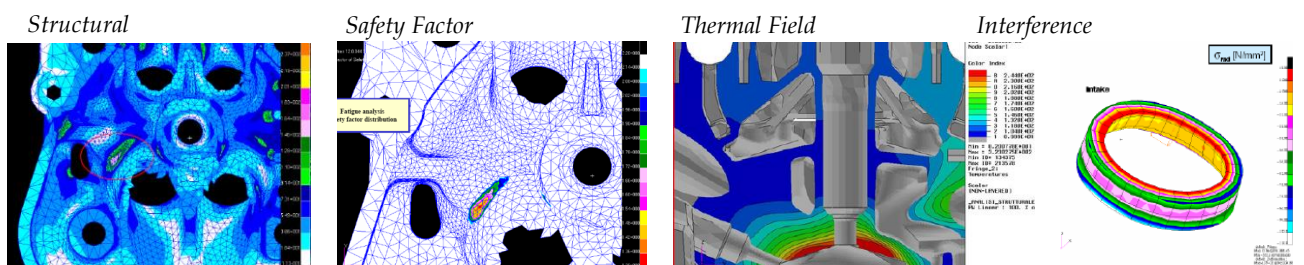
## FEM Analysis

The FE model must consider:

- loads due to gas pressure,
- dynamic loads due to distribution system,
- tightening loads which worsen the pressure load on the gasket,
- static load due to assembly with housing and valves,
- thermal load (steady state and transient)

The targets of the simulation are:

- structural analysis: von Mises stresses due to screws, pressure and thermal load,
- fatigue safety factor,
- temperature field,
- interference analysis.

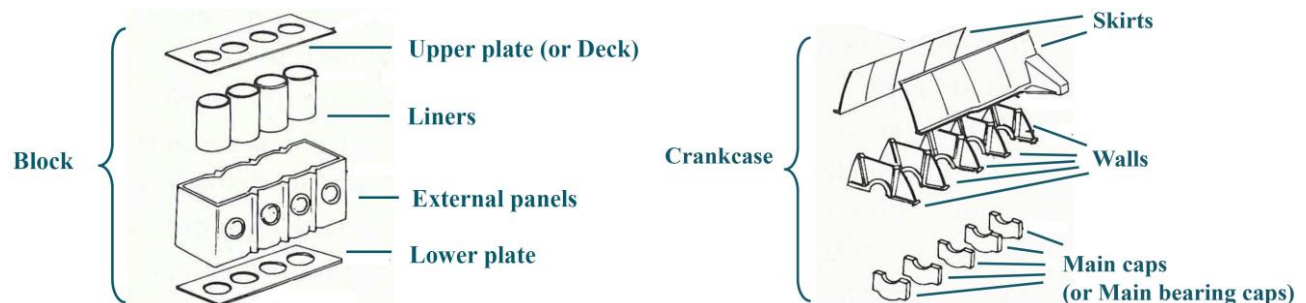
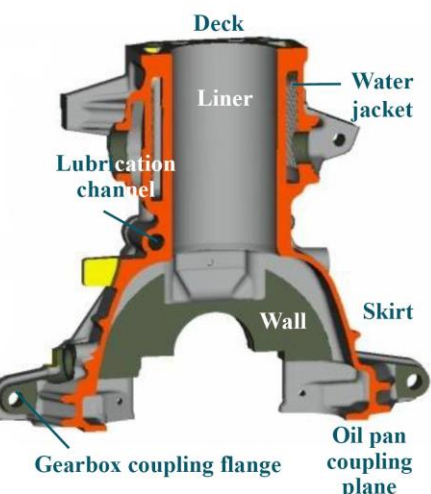


## 8. Cylinder Block

The cylinder block is the engine foundation and it can be designed as a single component mounted on engine vibration absorber to the chassis of the vehicle. It accommodates the liners, main bearings and all accessories.

The cylinder block includes an upper part named *block* and a lower part called *crankcase*:

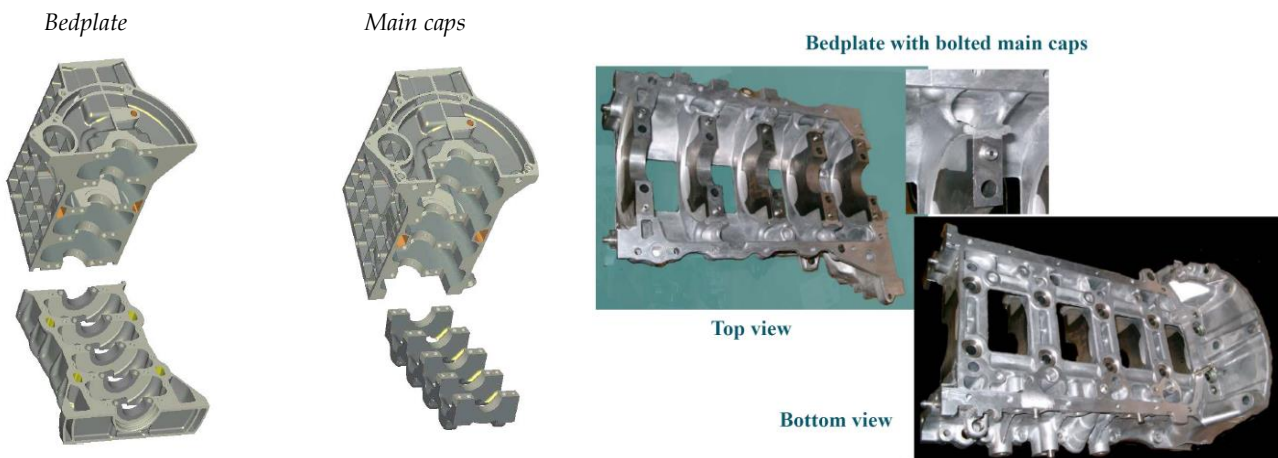
- Block, a single rigid assembly made up of liners and upper and lower gaskets,
- Crankcase, an open structure made up of skirts, walls and main bearing caps.



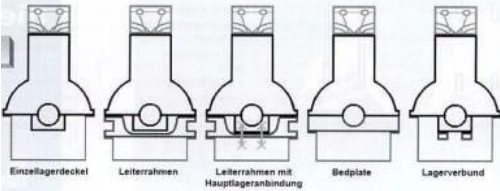
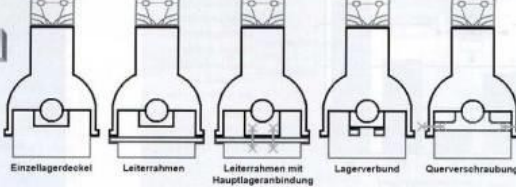
The geometry of the cylinder block is functional to the torsional stiffness. Different solutions are used to increase this stiffness:

- short or deep skirts,
- bearing beams,
- bedplate including all main caps

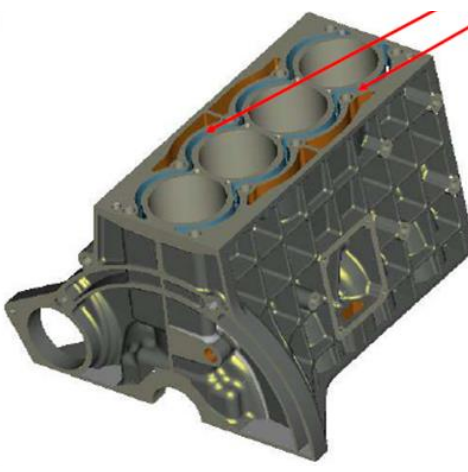
The bedplate solution provides the stiffest block structure, but it is more expensive; it is generally used in high pressure die case cylinder blocks to simplify the casting process. All this solution are resultant of a trade-off including stiffness, lightness and costs.



The skirts are positioned 5-6 mm far from the *guitar* so to accommodate the envelope of the crank rod revolution and to avoid oil pumping effect during crank rotation.

Short Skirt	Long Skirt
 <b>Einzellagerdeckel</b> <b>Leiterrahmen</b> <b>Leiterrahmen mit Hauptlageranbindung</b> <b>Bedplate</b> <b>Lagerverbund</b>	 <b>Einzellagerdeckel</b> <b>Leiterrahmen</b> <b>Leiterrahmen mit Hauptlageranbindung</b> <b>Lagerverbund</b> <b>Querverschraubung</b>
<ul style="list-style-type: none"> <li>- End at the center line of the crankshaft</li> <li>- Low problems about NVH</li> <li>- Oil pan is deep and can be resonant</li> </ul>	<ul style="list-style-type: none"> <li>- Extend 60-70 mm below the center line</li> <li>- Problems about NVH (behave as loudspeakers)</li> <li>- Oil pan is short and less resonant</li> <li>- Bedplate solution make the structure stiffer</li> </ul>

Another important design solution is the deck, which is the path of the coolant fluid circuit.

Open Deck	Close Deck
	
<ul style="list-style-type: none"> <li>- The coolant can freely flow up to the sealing surface</li> <li>- Commonly obtained by low cost casting (HPDC)</li> <li>- Difficulties to guarantee continuous sealing</li> <li>- Simplest solution if coupled with wet liners</li> <li>- Noise</li> </ul>	<ul style="list-style-type: none"> <li>- The coolant cannot freely flow up to the sealing</li> <li>- Requires expendable water jackets core (no HPDC)</li> <li>- Expensive if modified die casting process are used</li> <li>- Solution with cast-in liners are cheap</li> <li>- Higher structural stiffness</li> <li>- Perfect sealing is guaranteed</li> </ul>

## Material

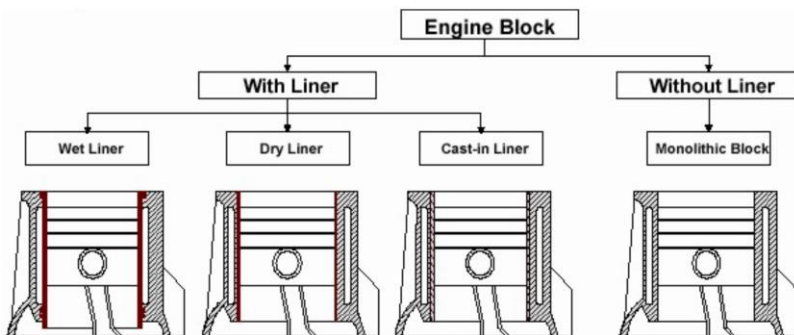
Usually, the material for the cylinder block are:

- Cast iron with Al-alloy bedplate,
- Hypereutectic Al-alloy ( $\text{Si} > 12\%$ ),
- Magnesium with Al-alloy inserts.

Magnesium structure allows to be 25% lighter than the conventional Al-alloy solution.

## Liners

Cylinder block can be *with* or *without* liners according to whether the liners are physically present (wet, dry or cast-in solution) or obtained by processing the internal part of the cylinder block itself. The difference between wet and dry liners stands in the direct contact with the coolant. Dry liners can also be built separately through cast-in and then inserted in the block housing.



The two most important parameters about the good functionality of the liner are:

- internal surface finishing since a good result highly reduce internal friction and increase the sealing effect with the piston,
- deformation of the longitudinal cylindrical surface that can be caused by high mechanical and thermal stresses

## Plateau Finishing

Plateau finishing uses spindle with diamond stone. The basic finishing creates pockets in the order of  $8\text{-}9 \mu\text{m}$  useful for the lubricant fluid.



Smaller pockets,  $2\text{-}3 \mu\text{m}$ , constitute the supporting surface on which the piston slides with respect the liner.

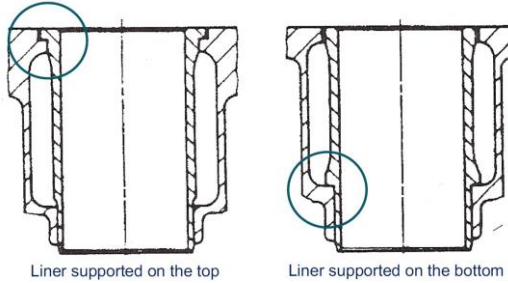
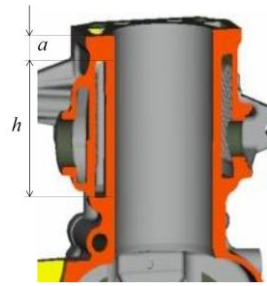
## Laser Finishing

Laser finishing uses laser to obtain a rifling with the desired dimensions and position of the pockets to achieve a desired lubrication structure. Different rifling and designed lubrication structure can be obtained.

Experimental analysis shows that laser finishing decreases the friction coefficient up to 60 % compared to Plateau. A further friction reduction can be achieved by decreasing the tangential load on the piston.

## Cooling

The liner cooling is guaranteed by the circulation of the coolant fluid around the liners along the water jacket that is located at the ring-land level of the piston. To stiffen the deck and to decrease the engine weight, the water jacket must be placed in lower position (increasing  $a$ ), while the length  $h$  must be reduced. A numerical CFD investigation is then needed to avoid engine warm-up problems.



The length support of the liner affects its performance. The design of the deck imposes certain solution; closed deck cylinder block admits upper collar support on the top, on the contrary the open deck liners have a lower collar support on the bottom. In high performance engines, wet liners are supported on the middle.

The optimal cooling solution is obtained with a circulation of the coolant fluid all around the liner circumference. However, this imposes an increasing of the distance between two adjacent liners (due to the presence of the liner material thickness + the water jacket). Because of the increase in longitudinal length, the cast-in liners are linked each other in the so-called twinned solution to save space.



## Mechanical Deformation

The liner transversal profile may deform under the action of screw forces. The deformation of the liner is experimentally measured (with a specific tool named *Talyrond*). An acceptable circumferential deformation is in the order of 20-30  $\mu\text{m}$ . Through the Fourier transform, one can identify the different order of deformation:

- 1<sup>st</sup> order      circle
- 2<sup>nd</sup> order      ellipse
- 3<sup>rd</sup> order      tri-lobed shape...

The mechanical deformation is affected by the position and depth of the threaded holes for the cylinder head fixing screws. To reduce this deformation, the cylinder head fixing screws are moved as outside as possible with respect to the liners.

## Types of Liners

Liners are produced in different type:

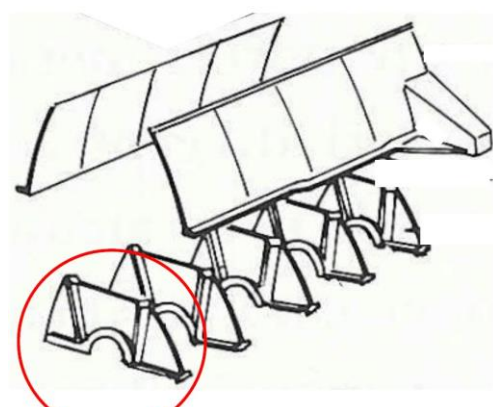
- |                          |  |
|--------------------------|--|
| • Cast-in                | made of Al-alloy with galvanic coating or hypereutectic Al-alloy     |
| • Sintered               | low dispersion of material and high material compositions            |
| • Bi-layer               | made of a lamellar cast iron in the internal and Al-alloy externally |
| • Metal Matrix Composite | casting technique with forms filled in laminar flow regime           |
| • Plasma coated          | plasma is sprayed to increase mechanical and tribological properties |
| • Ceramic coated         | Low Temperature Iron Titanate is applied to improve anti-friction    |

## Design Guidelines

### Wall

The wall and the main caps form the structure that support the crankshaft. Thus, the input force is the maximum resultant force  $F$  transmitted by the crankshaft. The force  $F$  can be assumed proportional to  $F_{g,max}$  or to  $F_{a,max}$  depending on the time instant. Also, one must consider the force of the screws (or studs) in the most stressed section.

$$F = \begin{cases} F_{g,max} = p_{max} \frac{\pi D^2}{4} \\ F_{a,max} = m_a \omega^2 r(1 + \lambda) \end{cases}$$



About the wall design, 3 different cross sections must be considered depending on how it is fixed.

Wall Fixed by Screws	Wall Fixed by Studs
$F_t = \frac{F}{2} \cos \alpha \quad \Rightarrow \quad \sigma_t^I = \frac{F_t}{A_{I-I}}$ $M_b = \frac{F}{2} \sin \alpha \cdot L \quad \Rightarrow \quad \sigma_b^I = \frac{M_b}{W_{I-I}}$ $\sigma_{eq} = \sigma_t^I + \sigma_b^I \leq \sigma_{adm}$	$F^*(1+k)$ $\frac{F^*(1+k)}{2}$ $\frac{F^*(1+k)}{2}$ <p>The cylinder head generates a force <math>F^*</math> such that:</p> $F^* = p_{max} \frac{\pi d_g^2}{4}$
$M_b = \frac{F}{2} L_1 \quad \Rightarrow \quad \sigma_b^{II} = \frac{M_b}{W_{I-I}}$ $\sigma_{eq} = \sigma_b^{II} \leq \sigma_{adm}$	<p>As for the cylinder head, the studs fixing pre-load must be multiply by <math>(1 + k)</math>, where the coefficient <math>k</math> is commonly equal to 0,5.</p> <p>The compressive stress has to be limited to the admissible compressive stress of the material:</p> $\sigma_c^{III} = \frac{F^*(1+k)}{A_{III-III}} \leq \sigma_{adm}$

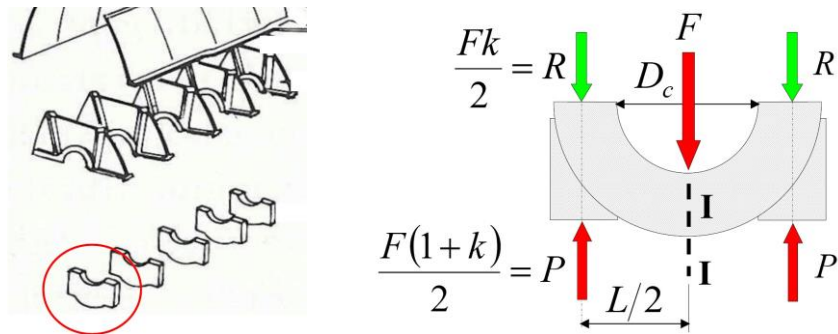
## Main Cap

The main caps are fixed to the wall. The load on the main caps depends on the arrangement in the engine architecture. Still, the maximum load that acts on each cap is proportional to the maximum gas force:

$$F = F_{g,max} = p_{max} \frac{\pi D^2}{4}$$

Also the main cap is fixed to the corresponding wall by means of screws with tightening load  $P$  which as usual must be corrected by the term  $(1 + k)$ . The resistance force  $R$  then results:

$$R = \frac{Fk}{2}$$



On the most stressed section (I-I), the bending moment is such that:

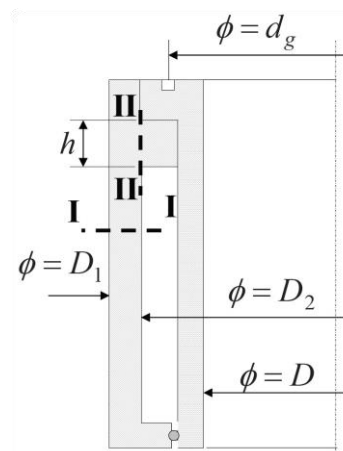
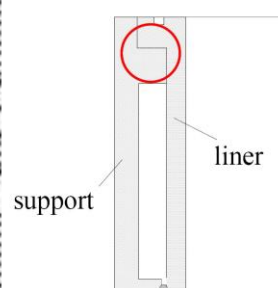
$$M_b = (P - R) \frac{L}{2} - \frac{1}{2} F \frac{D_c}{4}$$

in which the term  $FD_c/4$  is the bending moment produced by the elementary forces (generated by  $F$ ) acting on the half-circumference with diameter  $D_c$ . The consequent bending stress has to be limited to the admissible:

$$\sigma_b^l = \frac{M_b}{W_{I-I}} \leq \sigma_{adm}$$

## Liner Support

In case of press-fitted wet liners, the support and the liner are schematized in order to make the analytical calculation. The part highlighted in red is the *flange*.

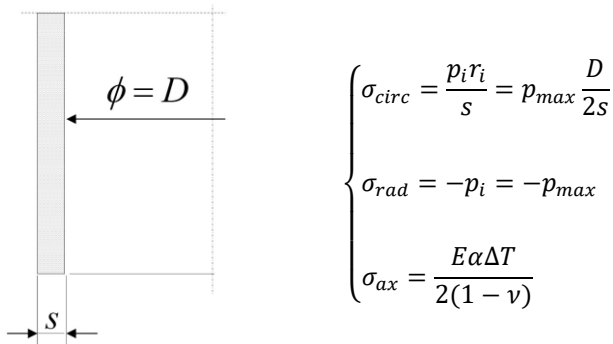


Also depending on the fixing system, the liner support undergoes to different stresses:

Liner Support Fixed by Screws	Liner Support Fixed by Studs
Subjected to <b>Tensile</b> in section I-I $\sigma_t^I = \frac{F}{A_{I-I}} = p_{max} \frac{D^2}{(D_1^2 - D_2^2)}$	Subjected to <b>Tensile</b> in section I-I $\sigma_t^I = \frac{F^*(1+k)}{A_{I-I}} = p_{max} \frac{d_g^2(1+k)}{(D_1^2 - D_2^2)}$
	Subjected to <b>Shear</b> in section II-II $\tau^{II} = \frac{F^*(1+k)}{\pi D_2 h} = p_{max} \frac{d_g^2(1+k)}{4D_2 h}$

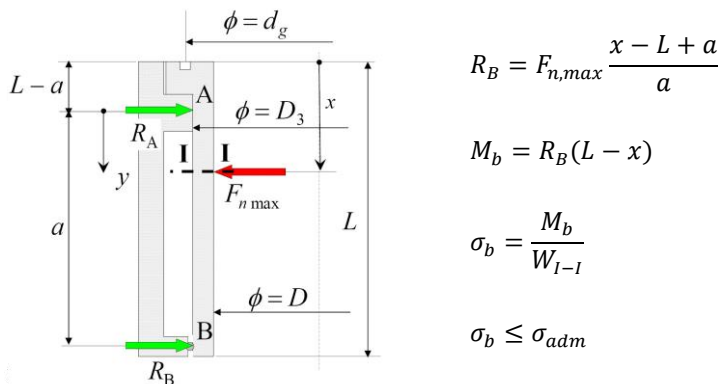
### Liner Wall

The liner wall is the liner internal surface and it can be studied as a thin pipe loaded by an internal pressure equal to the maximum gas pressure. From the Thin Tube Theory, the stress state on the liner wall is:



The equivalent stress (computed though Tresca or Von Mises) has to be lower than the admissible stress of the liner material:  $\sigma_{eq} \leq \sigma_{adm}$ .

Because of the normal force  $F_n$  transmitted by the piston, it is also required to verify the bending stress. The distance  $x$  represents the distance from the TDC in which  $F_n$  is maximum. This distance  $x$  can be evaluated in the crank-slider mechanism. From the equilibrium to rotation around point A, the analysis is:



## Liner Flange

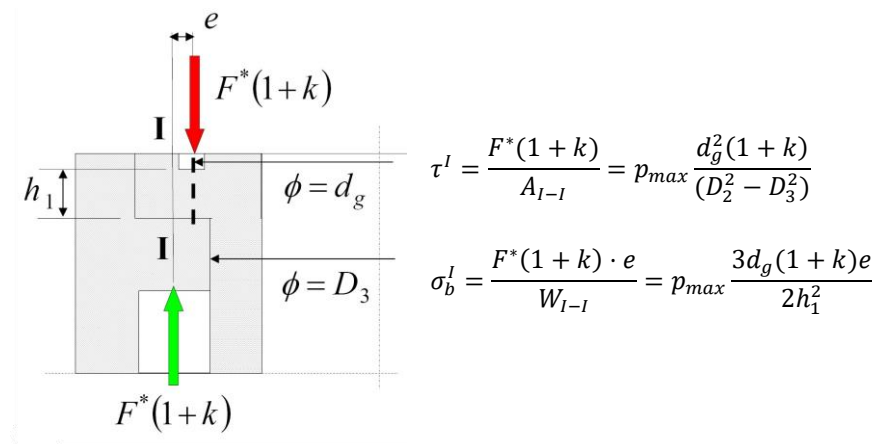
The liner flange is loaded by:

- tightening force produced by the cylinder head screws
- bending generated by misalignment between the gasket and the liner support

Considering the contact pressure  $p$  with the support collar equal to:

$$p = \frac{F(1+k)}{A} = p_{max} \frac{d_g(1+k)}{4h_1}$$

Thus, in section I-I, the shear and bending stresses are:



## Numerical Analysis (FEA)

In the FE model, the stresses on the cylinder block and the characteristics to analyze are:

- |                                     |  |
|-------------------------------------|--|
| • dynamic load from crank mechanism | fatigue, especially on main bearings,,                 |
| • dynamic load from balance system  | fatigue, especially on bearings of the balance shaft,  |
| • thrust load on the liner          | wear,  |
| • tightening of head screw          | liners distortion and incorrect pressure distribution, |
| • thermal load                      | liner distortion due to high thermal gradient.         |

In cylinder block FEA is possible to consider:

- Mechanical and thermal loads
- Static and dynamic loads
- Viscos-elastic sliding condition of material

The Static analysis allows to estimate stress condition, in particular on areas with important variation of geometry (potential cracks development), and fatigue behavior.

Dynamic analysis allows to verify the presence of coupled modes (bending, axial and torsional) and study the cylinder block behavior from NVH perspective.

## 9. Oil Pan

The oil pan can be a simple holder, but it can also have structural function:

- to increase the bending natural frequencies of the powertrain,
- to stiffen the link between engine and gearbox.



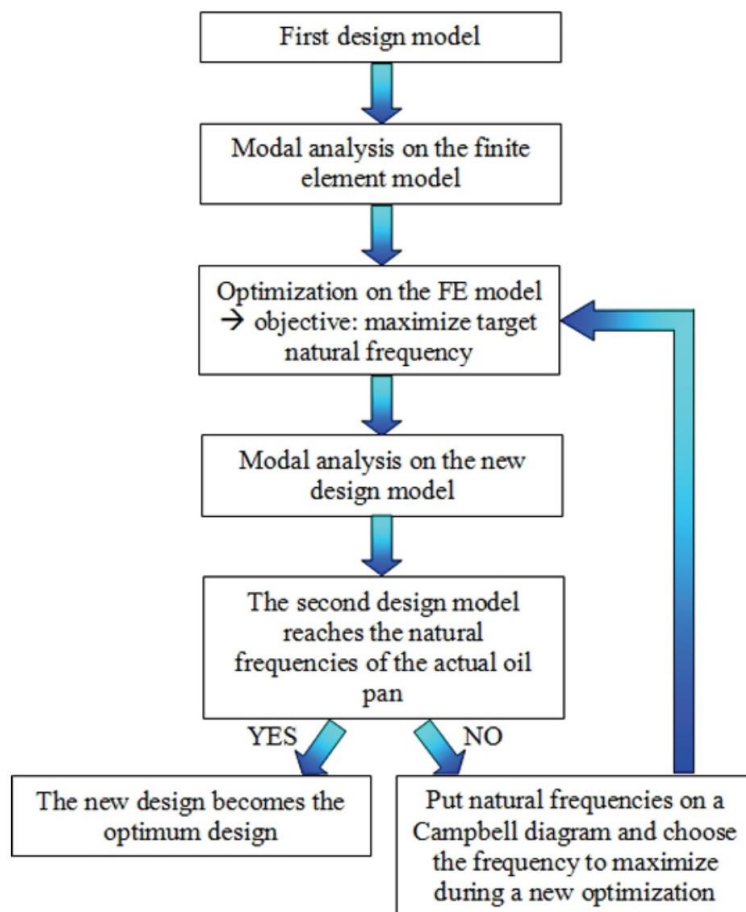
In case of structural function, the oil pan presents stiffening ribs that complicate the geometry.

The most used materials are steel sheet, double steel sheet or sandwich solution to minimize the panel acoustic emission. Al-alloy is mainly used for complex geometries, while mixed solution Al-alloy/Mg-alloy with steel sheet are focused on weight saving.

In oil pan design two conflicting goals can be highlighted: NVH performance and engine weight saving. In fact, the more the oil pan is stiff the more it is heavy.

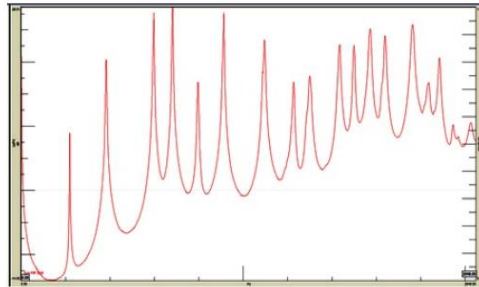
### Numerical Optimization – Modal Analysis

The proposal is useful to design a new oil pan, still with the same dynamics (natural frequencies) of the original and also improve weight saving. The optimum design follows this procedure:



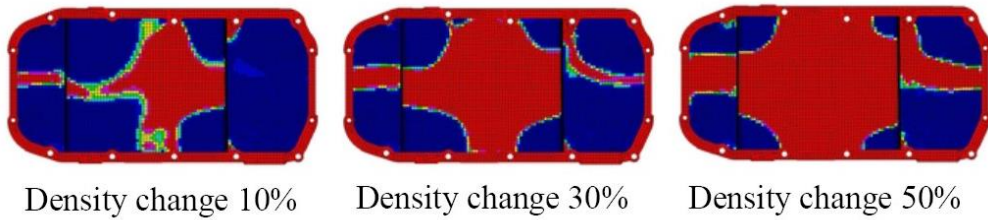
The Multi Input Multi Output (MIMO) modal analysis is performed in Test-Lab with suitable software. For example the experimental natural frequencies up to 1000 Hz obtained through an Experimental Modal Analysis (EMA) are:

<b>Mode</b>	1	2	3	4	5	6
<b>Freq.</b> EMA [Hz]	218	382	597	681	796	912



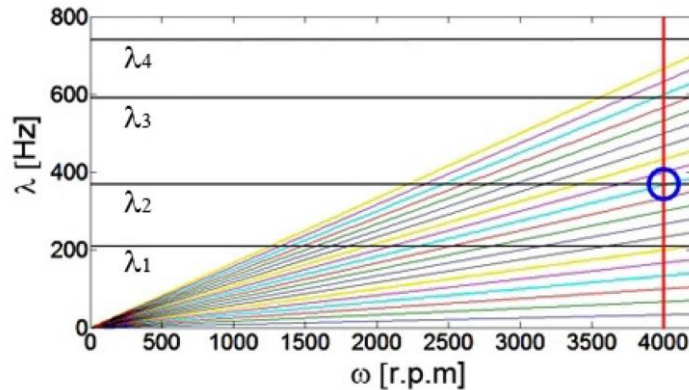
This result gives the target frequencies for the optimization design. The Numerical Modal Analysis is then performed on the FE model to compare the first design model with the original.

If the natural frequencies are lower, then it is required to optimize the model. To increase the natural frequencies, usually one increases the density material (thickness). In this way the material in zones in which is not *useful* about natural frequencies can be cut off and save weight.



Density change 10%      Density change 30%      Density change 50%

Assume that, despite the density increment, the frequencies are still lower. In this case, one must place the last obtained frequencies  $\lambda_i$  in a Campbell Diagram. Then one must choose the frequency to optimize (note that the oblique lines are the engine harmonics).



Once the process is validated (no intersection between oil pan natural frequency and engine harmonics at maximum engine speed), one can use this methodology to design a new oil pan with the same initial FE model. Usually using different material is the first step of a new design.

The final target of optimization is: save weight and increase natural frequency. The ultimate validation is given by the Campbell Diagram, that is: no intersection between natural frequency, max engine speed, and engine harmonics.

## 10. Thermo-Mechanical Fatigue

When dealing with fatigue phenomenon, it is necessary to distinguish between different cases:

- Mechanical fatigue      Isothermal
  - High Cycle Fatigue (HCF),      the test goes from thousands to millions cycles but the material remains in the elastic range (High Diagram),
  - Low Cycle Fatigue (LCF)      the test goes from up to  $10^4$  cycles and the loads overcome the yield strengths of the material (Wöller Diagram),
- Thermal Fatigue      Temperature varies cyclically decreasing mechanical properties. If the material is not able to deform, the stresses are similar to those of mechanical fatigue.

The Thermo-Mechanical Fatigue (TMF) cycle is a loading condition in which temperature and strain fields act simultaneously on a component. Therefore, in the TMF, thermal and mechanical cycles are superimposed in several combination: in phase (IP) or in phase opposition (OP). The factors to be considered for estimating TMF life are:

- material properties,
- mechanical deformation and deformation rate,
- temperature range,
- phase condition (IP, OP) between mechanical and thermal.

The main goal of TMF analysis are:

- prediction of material behavior under thermal and mechanical loads,
- definition of the main parameters involved in the component failure,
- estimation of the component residual life.

In test-lab the equipment needed to perform all kinds of analysis are:

- Vibrofore                          HCF test,
- Servohydraulic machine        LCF test,
- Oven                                Isothermal test,
- Induction heater                Thermal cyclic tests.



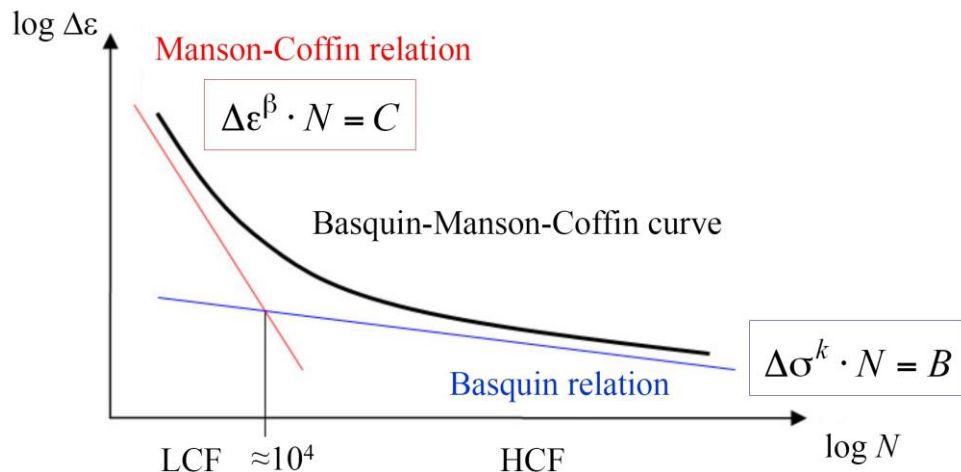
Back to the mechanical fatigue, the relations needed to describe the tests are as follows:

High Cycle Fatigue (HCF)	Low Cycle Fatigue (LCF)
<p>Stress-controlled and strain-controlled tests give almost the same result.</p> <p>Usually represented in Haigh Diagram.</p> <p><b>Basquin</b> relation correlates the stress <math>\Delta\sigma</math> to the number of cycle <math>N</math>.</p> $B = \Delta\sigma^k \cdot N$	<p>Strain-controlled tests characterize much better the behavior of the component.</p> <p>Usually represented in Wöhler Diagram.</p> <p><b>Manson-Coffin</b> relation correlates the stress <math>\Delta\varepsilon</math> to the number of cycle <math>N</math>.</p> $C = \Delta\varepsilon^\beta \cdot N$

The total strain range is the sum of thermal and mechanical strain:

$$\Delta\varepsilon_{tot} = \Delta\varepsilon_{th} + \Delta\varepsilon_{mech}$$

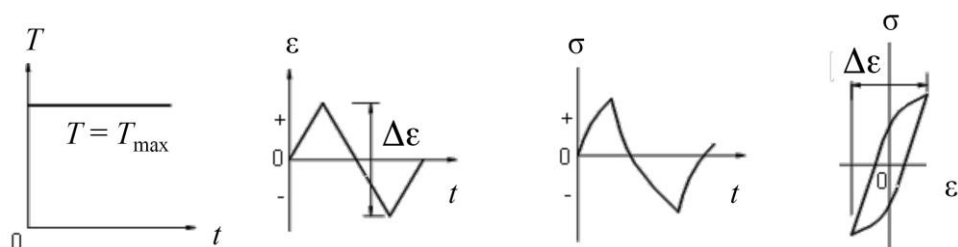
In which  $\Delta\varepsilon_{mech}$  is made up of the elastic contribution  $\Delta\varepsilon_{el}$  and the plastic contribution  $\Delta\varepsilon_{pl}$ . The general behavior is given by the empirical Basquin-Manson-Coffin curve, in which the damage is computed as function of the strain only. Still, creep and oxidation are neglected.



## Hysteresis

Starting with the **isothermal condition**, the testing temperature is constant and equal to the maximum temperature achievable  $T_{max}$ . The strain rate is imposed, thus obtaining the stress rate.

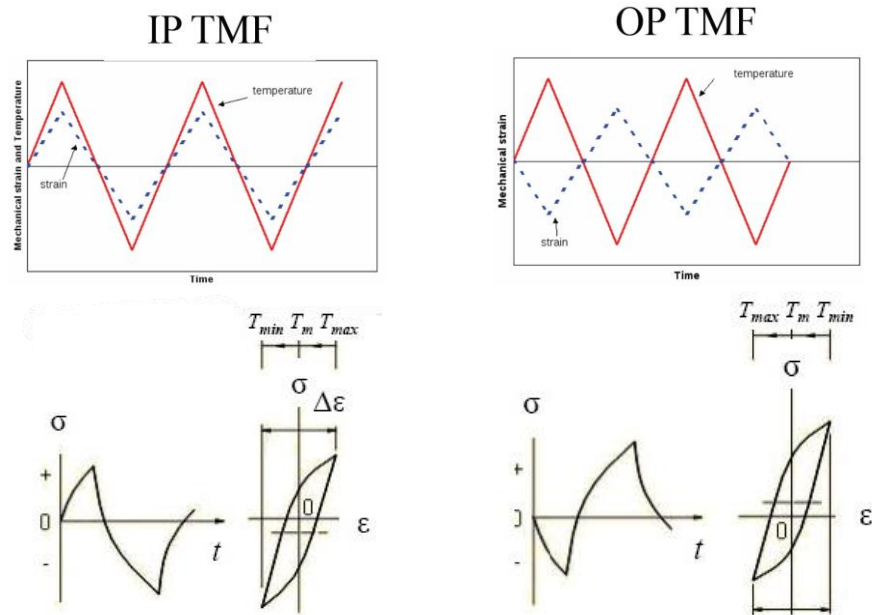
The hysteresis loop ( $\varepsilon\sigma$  graph) is obtained by combining together the strain and stress ranges. If the imposed strain is symmetric, then also the hysteresis loop is also symmetric with respect the origin of the  $\varepsilon\sigma$  axes.



On the contrary, in **thermo-mechanical fatigue**, the testing temperature varies cyclically between two fixed values. Here, strain cycles are independent from temperature. Thus, depending on the type of combination between the two cycles, one can obtain:

- In-Phase (IP) TMF tests max temperature and max strain are in the same time instant,
- Out-of-Phase (OP) TMF tests temperature is maximum when strain is minimum.

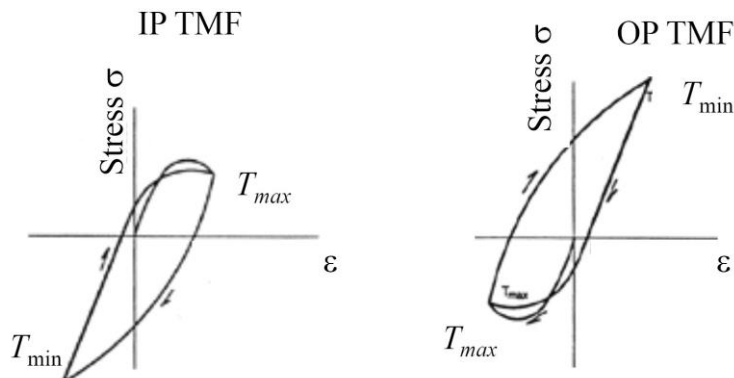
Usually, IP tests show a compressive mean stress ( $\sigma$  negative), whereas the OP tests show a tensile mean stress ( $\sigma$  positive).



Since in OP TMF is compressed when the temperature  $T$  is minimum, then this condition is more sensitive to oxidation effect because the oxide layer is formed at high temperature during the phase of mechanical compression. When the temperature decreases, the oxide layer becomes brittle and the subsequent phase of mechanical traction rapidly breaks the oxidized layer exposing new material to the subsequent oxidation.

The actual trend of the material shows an hysteresis loop shifted towards the compression field in IP and tensile field in OP. Definitely, OP condition is the most dangerous for the material failure. The related damages are:

- mechanical deformation; mechanical fatigue damage is due to hysteresis caused by loading condition,
- creep; visco-plastic deformation at high temperature.
- oxidation.



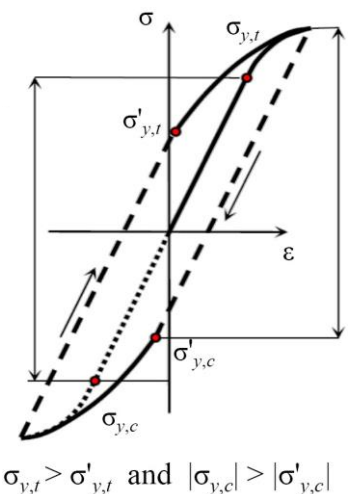
## TMF Fatigue Damage

### Baushinger Effect

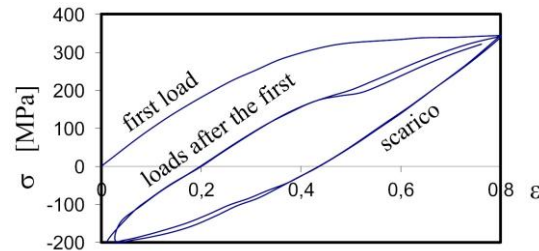
The Baushinger effect is a material behavior related to the first loading cycle: the yield stress of the material at the first load application is usually higher than the yield stress shown by the material during the successive hysteresis cycles.

Thus the consequence is a decrease of the compressive elastic limit after the first loading. Physically, the component remains permanently deformed at crystalline level and this generates material anisotropies.

At macroscopic level, these anisotropies decrease the elastic limit of the material.



### Cyclic Hardening/Softening



In general, the material hysteresis loops change with the increase of the accumulated number of cycles up to reaching a stable level that persists until failure.

In symmetrical strain-controlled tests (zero mean stress), the material can show two different behaviors in the not-stabilized-phase:

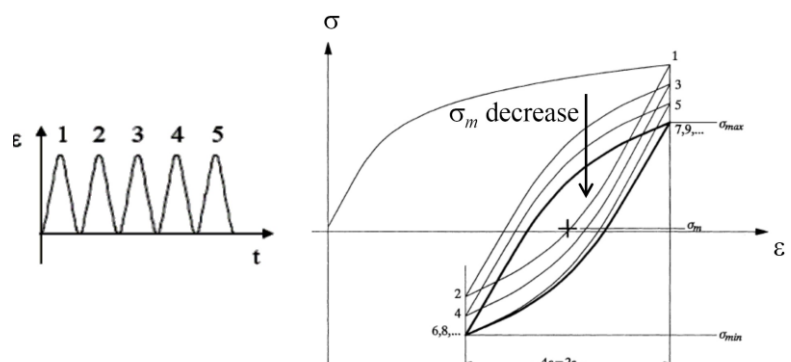
- cyclic hardening; the stress required to reach the imposed strain increases, as well as the elastic limit,
- cyclic softening; the stress required to reach the imposed strain decreases, as well as the elastic limit.

Material that suffer hardening are usually those without heat treatments whereas on the contrary, material that undergoes heat treatments or heavy plastic deformation, tend to soften cyclically.

### Shakedown Effect

In non-symmetrical strain-controlled tests (non-zero mean stress) in which the load exceeds the yield strength, when the load cycles have a positive mean stress, resulting the hysteresis loop tends to decrease the mean stress value towards zero. This is named *relaxation of the mean stress*.

High plasticization leads to a complete relaxation of the mean stress, whereas in low plasticization, the relaxation can be only partial.

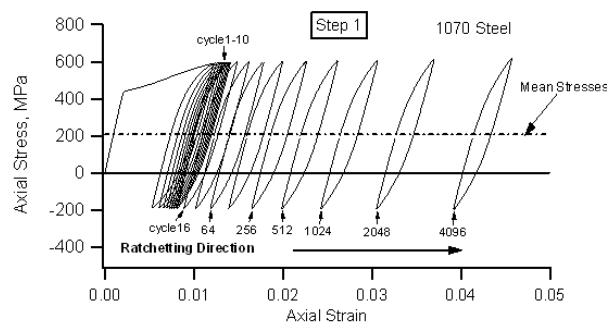


## Ratchetting

Ratchetting is an accumulation of plastic deformation that occurs in non-symmetrical strain-controlled test in which the load exceeds the material yield strength.

The effect is that the hysteresis loops are not closed but are constantly moving on the  $\sigma\epsilon$  plane towards increasing the value of the deformation in the direction of the applied mean stress. Certainly, ratcheting is a not stable behavior of the material.

In material that soften cyclically, ratcheting rate tends to increase, on the opposite, it tends to decrease in material that harden cyclically.



After a certain number of cycles, the phenomena stabilizes, and the hysteresis loop get closed (ratchetting rate goes to zero).

## Creep and Oxidation

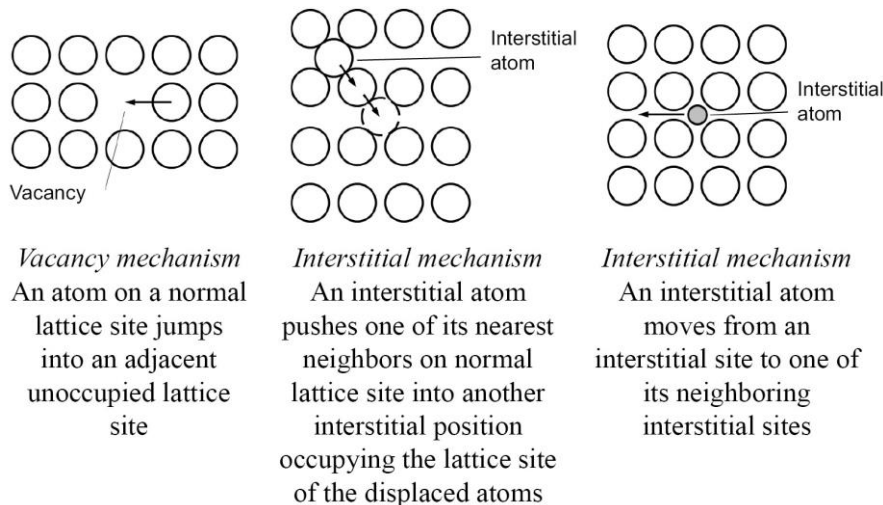
**Creep** is a time-dependent plastic deformation under constant load and temperature. Microstructures get rearranged by dislocation, aging and cavitation. Main causes of creep damage are:

- necking phenomena reduction of the resisting area,
- grain boundaries cavities and cracks,
- microstructural instability.

Empirical models provide simple formulas that correlate creep rate, stress, temperature and time for the estimation of the material behavior. These models are useful in the early step of design process.

**Oxidation** reactions are instead based on diffusion mechanism:

- vacancy mechanism,
- interstitial mechanisms.



## Residual Life Estimation

The component life (in terms of number of cycles to failure) depends on material and damage mechanism and can be estimated through the  $\Delta\varepsilon - N$  curves, or the corresponding mathematical methods. Any model to estimate the residual life is made of three parts:

1. material constitutive law      it correlates stress and strain,
2. damage model      describes the phenomena that cause damages,
3. failure criterion      express the limit value for the damage expression.

The thermo analysis computes the nodal temperatures which are then imposed to the structural analysis. This estimates the stresses and deformation caused by the superimposition of the temperature map and the mechanical cyclic load.

To get more details, the thermal load may be stationary or transient. The combination of the two gives the evolution in time of the component temperature field.

At the end of the simulation, the output is represented by the stress, strain, displacement, temperature and heat flow for each node of the FE model.

## Damage Models

The problem is that it is not clear how plastic deformation (fatigue), creep and oxidation interact each other and which is the predominant factor. Only with a correct damage model calibration it is possible to compute a correct estimation of the residual life of the component. Damage models are classified in *general* and *empirical*:

- General      based on physics of crack nucleation and propagation (complex),
- Empirical      based on experimental and microstructural observations (simpler).

Another important classification is based on the direction of the load:

- Uniaxial      single axial stress,
- Multiaxial      3D application with stresses in different locations.

All the models are a combination of General/Empirical and Uniaxial/Multiaxial analysis. The most known uniaxial TMF literature damage and failure criterion are reported in the table below:

<b>Basquin-Manson-Coffin</b>	Empirical Uniaxial	Damage is computed as a function of strain only. Failure criterion is the experimental curve.
<b>Neu-Sehitoglu</b>	General Uniaxial	Damage is the sum of creep and oxidation. Failure is based on cumulative damage assumption.
<b>Chaboche, BMW</b>	Empirical Uniaxial	Damage is the sum of mechanical fatigue and creep. Failure is based on cumulative damage assumption.
<b>Skeleton</b>	Empirical Uniaxial	Damage is function of the energy dissipated. Failure is based on a limit value of the dissipated energy.

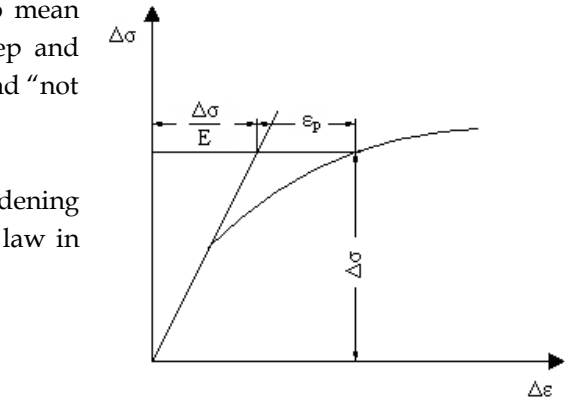
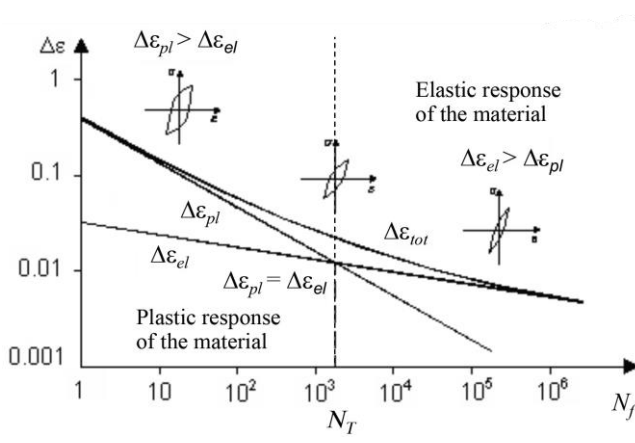
Several Multiaxial models (Von Mises, ASME code...) are based on the Basquin-Manson-Coffin relation.

### Basquin-Manson-Coffin Model

The Basquin-Manson-Coffin model is the simplest uniaxial damage model used both in LCF and in TMF with zero mean stress. Since this model neglects the contribution of creep and oxidation, then it is suitable for “not high temperatures” and “not long working time”.

The material is modeled according to a elasto-plastic hardening type (Hooke law in elastic range and Ramberg-Osgood law in plastic range). The total strain is the damage parameter:

$$\Delta\epsilon = \Delta\epsilon_{el} + \Delta\epsilon_{pl} = \frac{\Delta\sigma}{E} + \left( \frac{\Delta\sigma}{K'} \right)^{\frac{1}{n'}}$$



The parameters to be calibrated are the coefficients and exponents of strength and ductility to fatigue through experimental data from LCF and HCF tests. The failure criterion is directly defined by the experimental limit curve:

$$N_T = \frac{1}{2} \left( \frac{b-c}{\sqrt{\frac{\epsilon_f'E}{\sigma_f'}}} \right)$$

The residual life prediction is performed by imposing  $\Delta\epsilon$  (computed with FEA) and obtaining the number of cycles to failure  $N_f$ .

### Neu-Sehitoglu Model

Neu-Sehitoglu model is suitable for load histories with superimposed mechanical and thermal cycles. Thus, it is suitable from TMF application provided the experimental calibration of the parameters with respect the Basquin-Manson-Coffin model.

Here, the material is modeled as a viscos-plastic hardening type. The total damage (equal to the inverse of cycles to failure) is instead defined as the sum of the contribution of mechanical fatigue, creep and oxidation:

$$D = D^{fat} + D^{creep} + D^{ox} \Rightarrow \frac{1}{N_f} = \frac{1}{N_f^{fat}} + \frac{1}{N_f^{creep}} + \frac{1}{N_f^{ox}}$$

The fatigue damage is calculated through Basquin-Manson-Coffin, whereas creep and oxidation damage require extensive and expensive tests (due to calibration parameters).

### Chaboche, BMW Model

Chaboche models the material as a viscos-elastic type and the damage based on stress and in an implicit form. The differential formulation that neglect the oxidation damage:  $D = D^{fat} + D^{creep}$   
Here, the damage accumulation is linear and not superimposed; still, experimental calibration is required.

## Skeleton Model

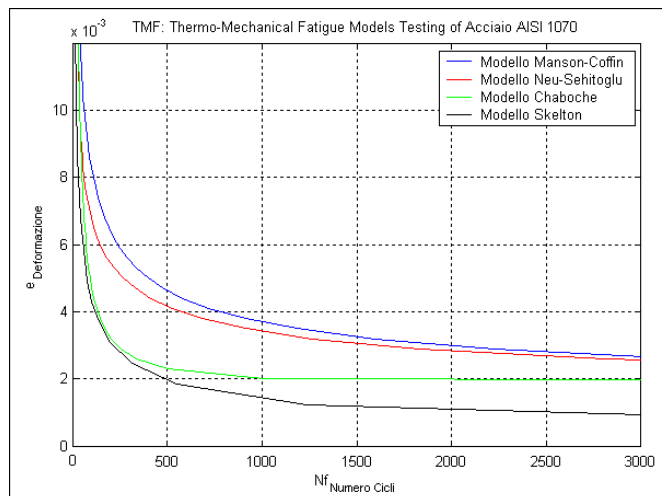
Skeleton model is based on an energy approach which correlates the energy dissipated in TMF condition to crack propagation. The residual life of the component is estimated as:

$$\frac{\text{total energy dissipated by the material up to failure}}{\text{energy dissipated by the component during its working condition}}$$

The total energy dissipated is computed as the total area of the hysteresis cycles up to failure. Since this is an energy approach method, there is difference between single and multiaxial condition.

Considering  $W_C$  as the total energy expenditure to reach the failure (material characterization) and  $W$  as the total energy expenditure after  $N$  cycles, then the number of cycles to failure (residual life) is:

$$N_f = \frac{W_C}{W}$$



## Multiaxial Models

Multiaxial models are developed to be used in LCF and TMF analyses of components where the stress state is generally multiaxial. Most of these models are based on the Basquin-Manson-Coffin model possibly corrected in case of non-zero mean stress.

All the multiaxial model calculate a uniaxial strain amplitude equivalent to the multiaxial condition acting on the component. This equivalent uniaxial strain amplitude is then introduced in the Basquin-Manson-Coffin model to estimate the cycles to failure.

Different model relies on different techniques to compute the equivalent uniaxial strain:

- von Mises Maximum octahedral strain criterion (exploits strain tensors),
- ASME code based on von Mises but computed starting from a strain variation,
- Sonsino-Grubisic damage is caused by the change of strain direction due to deformation,
- Kandill-Brown-Miller equivalent uniaxial strain amplitude starting from principal strains,
- Fatemi-Socie damage is controlled by shear strain component of maximum amplitude.

## 11. Exhaust Manifold

Exhaust manifolds collects exhaust gases from the exhaust valves and drive the gas to the turbine of the turbocharger, if present.

In modern diesel engines the common geometry is that of turbocharged engines: short runners with a unique outlet section to guide the exhaust gasses directly to the turbocharger.



### Material

The most used materials are:

- Steel AISI 409, 441, 429, 444, 321,
- Ductile cast iron Si-Mo, Si-Mo-Cr, Ni-Resist.

### Design Guidelines

The exhaust manifold is a component that highly influences the weight of the engine and the emissions quality. The working conditions are typical of a TMF condition and they are characterized by:

- thermal cycles due to hot flow of the gases, thermal expansion of the turbocharger,
- mechanical loads fastening and turbocharger weight.

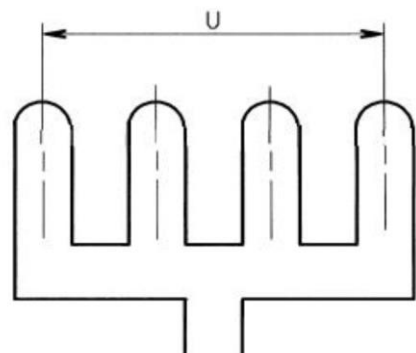
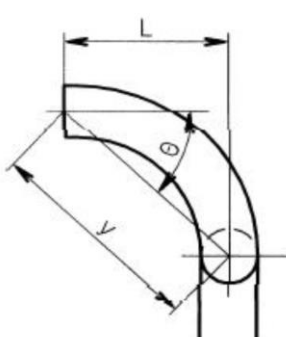
During the design procedure, the main requirements to be satisfy are:

- use of materials able to resist to thermal fatigue and oxidation,
- reduction of wall thickness to save weight and reduce thermal capacity for increase the fast heating,
- optimization of pressure waves avoiding interferences (turbocharger efficiency),
- reduction of thermal strains and distortions.

The procedure is semi-empirical. The geometry is modeled using beams loaded with force  $W$  and moment  $WL$ . The component main dimensions can be obtained using non-dimensional parameters. These non-dimensional parameters are:

- aspect ratio  $m$
- branch ratio  $b$
- offset ratio  $c$

$$m = \frac{L}{U}, \quad b = \frac{U}{y}, \quad c = \frac{L}{y}$$



To increase the manifold stiffness, the following items should be verified:

- small aspect ratio      it limits the amplitude of the deformation for internal runners
- large branch ratio
- large offset ratio

Numerical CFD analysis allows to define the second order approximation of the manifold geometry.

## Working Condition on the Test Bench

The typical working condition is an Out-of-Phase , Thermo-Mechanical Fatigue: OP TMF. This means that the exhaust manifold is loaded by a thermal and a mechanical load.

The thermal load is a cyclic non-isothermal load (engine characterization) and the heat exchange is:

- conduction      with cylinder head,
- convection      with environment.

The mechanical load is due to the mounting condition:

- bolts load,
- turbocharger weight,
- engine dynamic load.

Also it is required to perform a **thermal shock test** because of the extreme working conditions such as:

- fast speed regime variations,
- cooling, especially if manifolds are place in front of the cold air flux.

Finally, a leakage test must prove that no exhaust gases are quitting the manifold due to cracks.

## Material Behavior

Cast iron failure mainly regards:

- material temperature resistance      for high temperature LCF,
- crack propagation      for high temperature resistance cast iron.

Overall, the LCF behavior of the high resistance cast iron depends on the temperature. Indeed, the cast iron tends to:

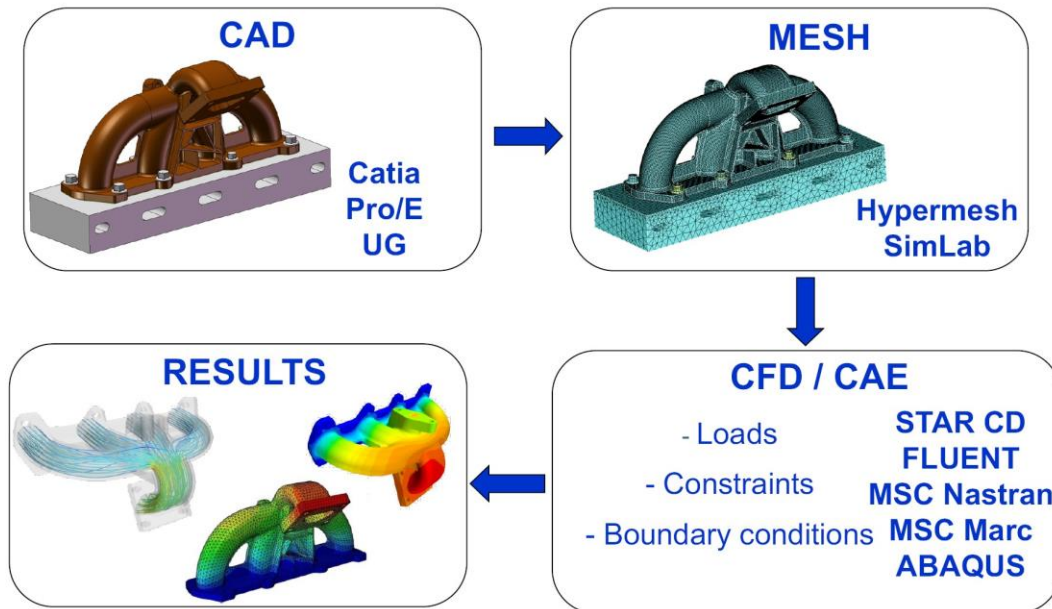
- cycle hardening      @ low and medium temperature      500°C ,
- cycle softening      @ high temperature      800°C .

The damage models are based on Basquin-Manson-Coffin and Skeleton models of a commercial Si-Mo-Cr cast iron. However, creep are generally neglected while oxidation would require more detailed models.

## Residual Life Estimation – FEA Analysis

The main purpose of FEA and TMF study is to predict the critical areas of the exhaust manifold in terms of structural integrity, and the estimation of the number of cycles to failure  $N_f$ .

The procedure follows this general scheme:

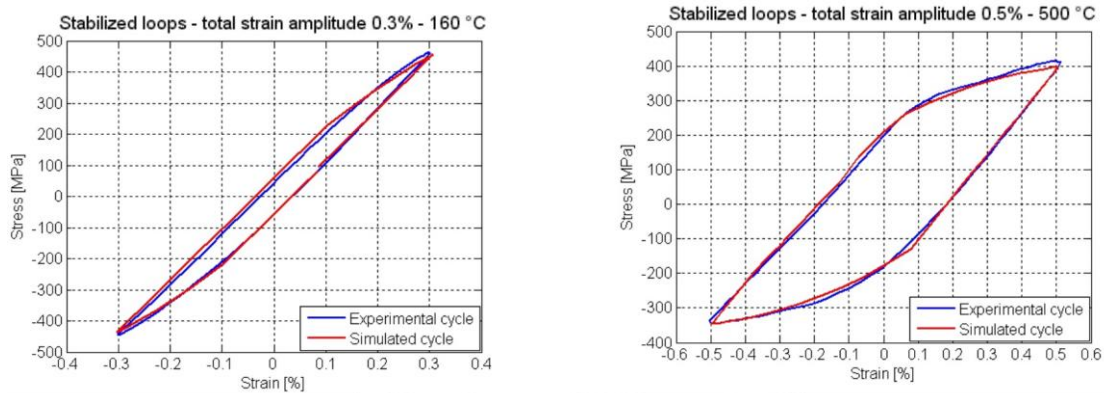


### FEA

In the Finite Element Analysis phase, two simulations must be performed:

- Thermal transient analysis      temperatures and nodal temperatures values after the cycle,
- Structural transient analysis      stress and strain due to bolt and then due to thermal expansion.

The temperature maps computed in the thermal analysis are then superimposed to the mechanical results. After the calibration, the comparison between experimental and simulated must prove that hysteresis loop variation is acceptable.



After the FEA, one can focus on the time evolution of all the variables of interest such as stresses, strains, nodal temperatures, etc.

## Multiaxial Damage Model

Also, multiaxial damage model are exploited in temperature ranging between 160°C and 800°C. This is possible by calibrating the parameters (four) of the Basquin-Manson-Coffin model. However, since this last model does not consider temperature-dependent relation, then one must calibrate the parameter for each temperature under investigation.

Residual life values must be computed for each critical FR detected in structural FEA.

Usually, the most probable area where the fatigue crack may nucleate and propagate is then reinforcement rib between exhaust manifold main collar and external runner.

